

# ANALYZING TRANSFORMER DYNAMICS AS MOVEMENT THROUGH EMBEDDING SPACE

Sumeet S. Singh   
 Turnitin  
 Oakland, CA 94612, USA  
 ssingh@turnitin.com

## ABSTRACT

Transformer language models exhibit intelligent behaviors such as understanding natural language, recognizing patterns, acquiring knowledge, reasoning, planning, reflecting and using tools. This paper explores how their underlying mechanics give rise to intelligent behaviors. We adopt a systems approach to analyze Transformers in detail and develop a mathematical framework that frames their dynamics as movement through embedding space. This novel perspective provides a principled way of thinking about the problem and reveals important insights related to the emergence of intelligence:

1. At its core the Transformer is a Embedding Space walker, mapping intelligent behavior to trajectories in this vector space.
2. At each step of the walk, it composes context into a single composite vector whose location in Embedding Space defines the next step.
3. No learning actually occurs during decoding; in-context learning and generalization are simply the result of different contexts composing into different vectors.
4. Ultimately the knowledge, intelligence and skills exhibited by the model are embodied in the organization of vectors in Embedding Space rather than in specific neurons or layers. These abilities are properties of this organization which in turn is defined by the model architecture and parameters.
5. *Attention's* contribution boils down to the *association-bias* it lends to vector composition and which influences the aforementioned organization. However, more research is needed to ascertain its significance.
6. The entire model is composed from two principal operations: data independent *filtering* and data dependent *aggregation*. This generalization unifies Transformers with other sequence models and across modalities.

Building upon this foundation we formalize and test a *semantic space theory* which posits that embedding vectors represent semantic concepts and find some evidence of its validity.

## 1 INTRODUCTION

Since their introduction Transformers (Vaswani et al., 2017) have made very rapid progress in the NLP domain (Devlin et al., 2019; Liu et al., 2019; Reimers & Gurevych, 2019; Raffel et al., 2020; Brown et al., 2020) and subsequently in Vision-Language (Chen et al., 2020; Dosovitskiy et al., 2020; Ramesh et al., 2021a; Alayrac et al., 2022; Lu et al., 2022; OpenAI, 2023) as well as multimodal-language domains (Reed et al., 2022; Driess et al., 2023; Girdhar et al., 2023). Initial applications of Transformers started in the sequence modeling realm where a lot of progress had already been made across modalities by RNNs, LSTMs (Hochreiter & Schmidhuber, 1997b; Stollenga et al., 2015; Kalchbrenner et al., 2015) and CNNs. Applications generally fell into three categories: 1) Autoregressive generation or masked denoising (Graves, 2013; van den Oord et al., 2016c;b; Theis & Bethge, 2015a;b; van den Oord et al., 2016d), 2) Sequence classification and 3) Sequence to Sequence transduction (Sutskever et al., 2014; Cho et al., 2014; Donahue et al., 2015;

van den Oord et al., 2016a; Kalchbrenner et al., 2016; Johnson et al., 2016). The key capability underlying these impressive results was the ability to estimate joint sequence probabilities for a task. However, not much investigation was done into how the hidden layers produced these probabilities. Later, *attention* was introduced (Bahdanau et al., 2014; Ba et al., 2014; Mnih et al., 2014; Xu et al., 2015) as a way of dealing with long-range dependencies and became standard practice for sequence modeling. Attention was described as a means for a model to select relevant parts of a context while de-emphasizing the irrelevant ones. However, doing so requires deciding what’s relevant and yet relevance was never explicitly modeled. It was hypothesized that the neural network learnt relevance on its own but this was never proven. Also, the name *attention* anthropomorphizes the mechanism, leading to unintended misconceptions. We hope to fix that in this paper by providing a mechanistic explanation of *attention*. Moving on, large language models (LLMs) advanced the state of art by generalizing to unseen tasks via zero and few-shot learning (Brown et al., 2020; Chowdhery et al., 2022). This was soon followed by advanced prompting techniques like chain-of-thought (CoT) prompting (Wei et al., 2022b; Kojima et al., 2023) and then just plain multi turn conversations made possible by instruction-tuned LLMs (Ouyang et al., 2022). Zero-shot or conversational prompting makes it appear as if Transformers understand natural language instructions and carry them out to the extent that claims have been made that they have Theory of Mind ability (Kosinski, 2023). Examples of few-shot learning make it appear as if the Transformer learns and recognizes patterns on the fly. CoT prompting makes it appear as if Transformers can think and explain themselves in natural language. Very impressive intelligent capabilities have been demonstrated in the NLP and vision-language areas e.g., prompt based source code generation (Chen et al., 2021), description based realistic image generation (Ramesh et al., 2021b), freeform conversations (OpenAI, 2023) and a variety of unexpected capabilities deemed as the beginnings of AGI (Bubeck et al., 2023; Wei et al., 2022a). And most recently, LLMs are being trained to act as autonomous agents, being able to observe, plan, reason, reflect, use external tools & APIs and act (Schick et al., 2023; Yao et al., 2023; Karpas et al., 2022; Park et al., 2023) even in a multimodal space (Liang et al., 2023; Lu et al., 2023). However, as Brown et al. note: *understanding precisely how few-shot [and zero-shot] learning works is an important unexplored direction for future research*. This paper attempts to answer this question; specifically we explore how intelligent behaviors arise from the underlying mechanics of Transformers. Expanding our earlier work “The Transformer Algorithm” Singh (2021) we analyze Transformer architecture and activations :

1. Mathematically formalize an embeddings-space centric framework (sec. 2.1).
2. Cast the dynamics of decoding in this framework (sec. 2.2).
3. Reinterpret Transformer layers in this new light (sec. 2.3).
4. Unearth insights that significantly advance our understanding of Transformers (secs. 2.2.1 and 3)
5. Test a semantic interpretation of embeddings (sec. 5).

The source code for visualizations of all open-source models in this paper is available here<sup>1</sup>.

## 2 AN EMBEDDING SPACE CENTRIC FRAMEWORK

While various Transformer architectures exist, they broadly categorize into three types: 1) The T5 (Raffel et al., 2020) style encoder-decoder, 2) GPT3 (Brown et al., 2020) style decoder only and 3) BERT (Devlin et al., 2019) style encoder only architecture. Since we’re interested in generative decoding, we focus on the first two architectures only and since the encoder-decoder architecture is a superset of the other two, we shall refer to the diagram of Figure 1. In this section we will redefine these architectures within our embedding space centric framework.

### 2.1 THE EMBEDDING SPACE

Formally, an embedding vector is a real vector  $e \in \mathbb{R}^D$  where  $D = d_{model}$  is the hidden size of the Transformer. Vectors are themselves composed from a sequence of one or more token embeddings

<sup>1</sup>Visualizations source code: <https://github.com/Turnitin-AI-Research/tta-paper>

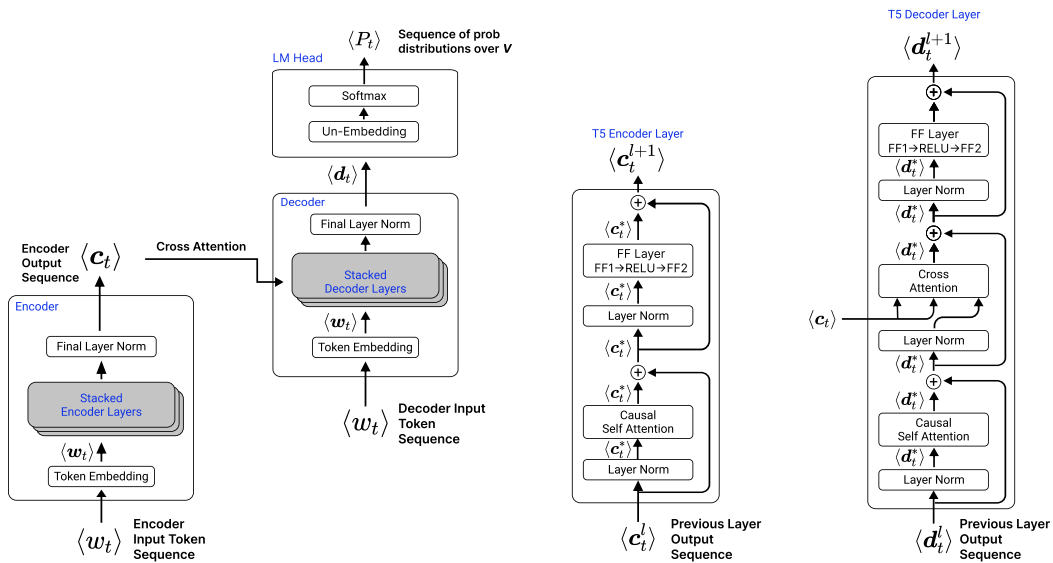


Figure 1: Architecture of a T5 Transformer. Encoder and decoder stacks (left), encoder layer (middle) and decoder layer (right).  $c_t^*$  and  $d_t^*$  denote intermediate vectors that don't have a particular name.

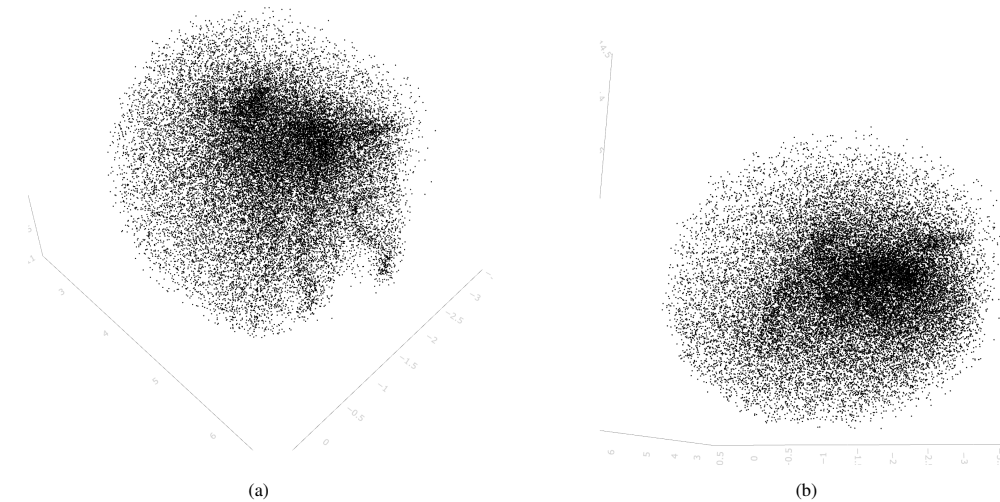


Figure 2: a) and b): Perspectives of 3D UMAP projections of the set of token embedding vectors  $\mathbb{V}$  trained with negative inner-product as the distance metric. The vectors are obtained from a t5-small model fine-tuned with few-shot examples of freeform answer grading. The 3d space organizes in a roughly spherical shape because vector magnitudes are bounded and the distance between vectors is governed largely by their angular distance.

and / or other composite vectors i.e.,  $e = f(\langle e_i \rangle)$  where  $e, e_i \in \mathbb{R}^D$  and  $f$  is a composition function implemented by the model, a layer or a sub-layer. For convenience, vectors produced inside the encoder and decoder stacks are denoted as  $c$  and  $d$  respectively. The Embedding Space is the topological space  $\mathbb{S} = \mathbb{R}^D$  occupied by embedding vectors with inner-product being its similarity metric (fig 2). While word embeddings and their compositionality are well established ideas (Bengio et al., 2003; Mikolov et al., 2013b; Cho et al., 2014; Reimers & Gurevych, 2019) we extend them in the following ways: 1) All size  $D$  hidden activations are considered as vectors  $\in \mathbb{S}$ . This includes all token embeddings, inputs & outputs of the encoder & decoder stacks, individual layers, summation points within layers and layer norm'd activations within layers as well (marked on Fig. 1 as  $w_t, c_t, c_t^*, d_t$  and  $d_t^*$ ). 2) Layers and attention blocks are cast as n-ary operators ( $f : \mathbb{S}^n \rightarrow \mathbb{S}$ ) in the Embedding Space while some sub-layers are cast as 1-ary operators ( $f : \mathbb{S} \rightarrow \mathbb{S}$ ) (section 2.3.1). Since they are self-mapping, the operators can be chained together to yield new operators. This enables framing the en/decoder stacks and the entire model as n-ary operators (section 2.3) in  $\mathbb{S}$ . Further, we reason that internal (size  $D$ ) activations as stated above are in fact embedding vectors because if this was not true, the Transformer would not be able to coherently: 1) Sum vectors across (sub)layers via residual connections, 2) Compare vectors between the input and output layers; this happens implicitly in the Transformer when vectors output from the topmost layer are multiplied with the output embedding matrix to obtain word logits. When the output and input embedding matrices are tied (as is the case with all the foundational models we referenced), this amounts to an inner-product i.e., comparison between output and input embeddings (since inner-product is the similarity metric), 3) Export encoder activations into all layers of the decoder via. cross-attention or 4) Sum outputs of attention heads of a layer<sup>2</sup> For all of these operations to be coherent, the vector dimensions must have the same *meaning* through the (sub) layers and stacks. As an aside, note that vectors are also being compared against each other via inner-product - the similarity metric - inside the attention blocks. Therefore all layers of both the encoder and decoder are operators in  $\mathbb{S}$ . Elhage et al. (2021) indirectly support this viewpoint via their concept of a "residual stream", a common information channel which all Transformer layers read and update. RNNs similarly, update a residual state vector at each step and layer. Geva et al. (2022) and Dar et al. (2022) also posit that all layers operate in the same space although they are referring to a Vocabulary Space.

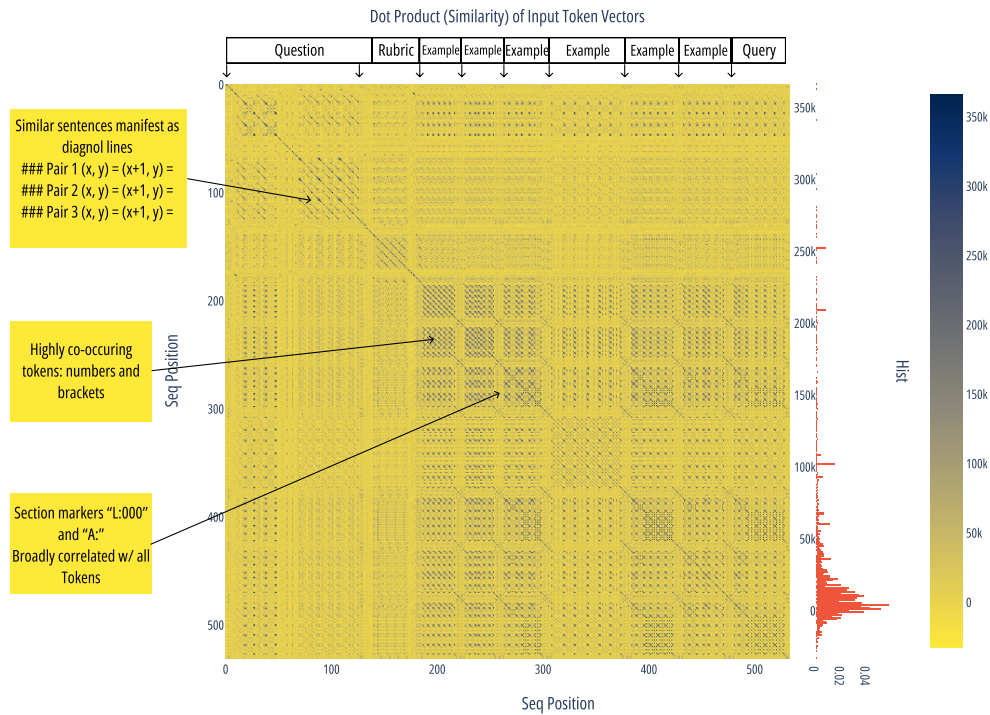
**Discussion** This is an important result because it implies that all layers of the Transformer operate at the same level of abstraction. It contradicts the prevailing view that higher layers of a neural network operate at progressively higher levels of abstraction which, the above analysis does not support at all. As an aside, this fact makes it very convenient to interpret hidden activations and weights via nearest neighbor analyses (Fig. 3).

## 2.2 THE DECODING WALK

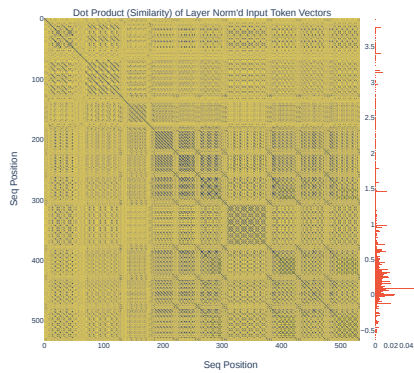
In this section we shall analyse causal decoding within this framework. Later sections will delve into the layers. As a reminder causal decoding entails predicting the next token given an input token sequence. In the case of an encoder-decoder architecture, the input sequence is a concatenation of the encoder and decoder inputs, whereas in the case of a decoder-only architectures there's only the decoder input<sup>3</sup>, part of which may itself have been generated via causal decoding. Sequence positions, also called time steps, start at 1 and are denoted by  $t$  or  $i$ . An analysis of causal decoding

<sup>2</sup>Multi-headed attention can be trivially refactored as the sum of independent attention paths. See A.1.

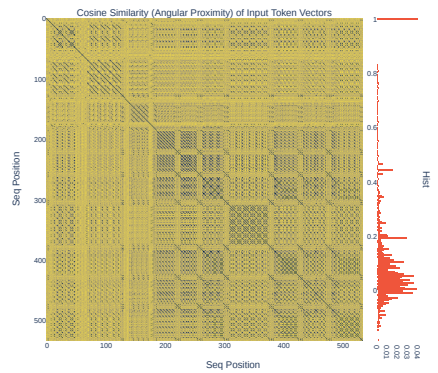
<sup>3</sup>Causal decoding does not apply to encoder-only architectures.



(a)



(b) Similarity after Layer Norm



(c) Cosine Similarity i.e., Angular Proximity

Figure 3: (a) Similarity map of token embedding vectors of a few-shot sample. The t5-small model was trained with structured few-shot examples on an answer grading task: starting with a question, then a scoring rubric, followed by 6 graded answers and finally a query answer whose grade the model is expected to generate. Formatting tokens that mark section boundaries (such as ‘Q:’, ‘A:’ and ‘L:000’ resp. for question, answer and label) co-occur weakly with all tokens and therefore form light bands. Highly co-occurring tokens like numbers and brackets form dark clusters. Thus the model appears to recognize the formatting pattern of the few-shot sample. The pattern is more pronounced after vectors are layer-norm’d in layer 1 (b) or compared with cosine-similarity (c); indicating that co-occurring / associated vectors cluster together by angular distance. Additional maps of frozen pretrained models are shown in the section A.2.

in this light yields equations 1 - 15. Please examine those equations.

$$\begin{aligned}
 w_t &\equiv \text{input token id at position } t ; t \geq 1 & (1) \\
 \mathbf{V} &\equiv \text{token embedding matrix ; size } V \times D & (2) \\
 \mathbb{V} &\equiv \{\mathbf{w}_i\}_{i=1}^V \subset \mathbb{S} ; \text{set of all token embedding vectors} & (3) \\
 \mathbf{w}_t &\equiv \text{word embedding vector of } w_t & (4) \\
 &\equiv \mathbf{V}_{w_t, :} ; \text{row } w_t \text{ of } \mathbf{V} & (5) \\
 \langle \mathbf{w}_i \rangle_1^t &\equiv \text{embedded input sequence from position 1 through } t & (6) \\
 &= \text{concated encoder and decoder inputs in case of encoder-decoder arch} \\
 f_{\Sigma; \theta} &: \mathbb{V}^n \rightarrow \mathbb{S} ; \text{causal composition function characterizing the model} & (7) \\
 \mathbf{d}_t, \mathbf{d}_{\langle \mathbf{w}_i \rangle_1^t} &\equiv \text{decoding vector ; output vector of decoder at position } t & (8) \\
 &= f_{\Sigma; \theta} \left( \langle \mathbf{w}_i \rangle_1^t \right) ; \text{causal composition} & (9) \\
 \langle \mathbf{d}_i \rangle_1^t &\equiv \text{decoding walk ; the sequence of decoding vectors through position } t & (10) \\
 P_t, P_{\langle \mathbf{w}_i \rangle_1^t} &\equiv \text{probability distribution over } \mathbb{V} \text{ output by the model at step } t & (11) \\
 &= \text{softmax} \left( \mathbf{d}_t \mathbf{V}^T \right) ; \text{the Logits Layer} & (12) \\
 &= \text{softmax} \left( \mathbf{d}_t \odot \mathbb{V} \right) ; \odot \equiv \text{inner product} = \text{similarity metric of } \mathbb{S} & (13) \\
 &= \text{softmax} \left( f_{\Sigma; \theta} \left( \langle \mathbf{w}_i \rangle_1^t \right) \odot \mathbb{V} \right) & (14) \\
 \mathbf{w}_{t+1} &\sim P_t ; \text{the decoding process} & (15)
 \end{aligned}$$

The transformer’s encoder and decoder stacks together can be cast as a composition function  $f_{\Sigma; \theta}$  that composes a sequence of token vectors  $\langle \mathbf{w}_i \rangle_1^t$  into a single vector representation  $\mathbf{d}_t \equiv \mathbf{d}_{\langle \mathbf{w}_i \rangle_1^t} \in \mathbb{R}^D$  (eqns. 7 - 9). Thus,  $f_{\Sigma; \theta}$  populates  $\mathbb{S}$  with the set  $\{\mathbf{d}\}$  of representations corresponding to all possible input sequences  $\{\langle \mathbf{w}_i \rangle\}$ . The generative decoding process generates a sequence one token at a time by sampling a token embedding vector  $w_{t+1}$ <sup>4</sup> from probability distribution  $P_t$  which was produced by the model at position  $t$  (eqn. 15). Now since  $P_t$  is a function of the previously traversed path  $\langle \mathbf{w}_i \rangle_1^t$  (eqn. 6 and 14), it follows that the decoding process is a non-Markovian random walk in  $\mathbb{S}$ . We denote the sequence of output vectors produced by this process as  $\langle \mathbf{d}_i \rangle_1^t$  and term it the *decoding walk* (eqn. 10).

**Organization of Embedding Space** Next, note that  $P_t$  is a function of the inner-product between  $\mathbf{d}_t$  and all the token vectors  $\mathbf{w}_i$  in  $\mathbb{V}$  (equations 3 and 13) i.e., the relative location of  $\mathbf{d}_t$  in Embedding Space<sup>5</sup> characterizes the probability distribution of the next token which in turn determines the *decoding walk* which in turn determines the generated sequence  $\langle \mathbf{w}_i \rangle$ . We term the placement of all possible embedding vectors produced by the model i.e.,  $\{\mathbf{e}\} \cup \mathbb{V}$  in  $\mathbb{R}^D$  as the *organization* of  $\mathbb{S}$ <sup>6</sup>

### 2.2.1 THE EMERGENCE OF INTELLIGENCE

Therefore given a fixed decoding procedure, the *organization* of  $\mathbb{S}$  completely defines decoding walks. Since all the knowledge, intelligence & skills expressed by the model are the result of *decoding walks*, it follows that these abilities are embodied in the *organization* of  $\mathbb{S}$ . Also, the abilities are emergent in the classical sense since they are a property of the system, not specific parts. Mechanically speaking, these abilities are determined by the same factors that determine the *organization* of  $\mathbb{S}$  viz. 1) the information capacity of  $\mathbb{R}^D$ ; which increases with  $D$ , 2) the *organization* of learnt token embeddings  $\mathbb{V}$  and 3) the vector composition function  $f_{\Sigma; \theta}$  which is defined by model architecture and parameters. Therefore, the question “how much knowledge can you pack into the parameters of a language model” (Roberts et al., 2020) can be reworded to “how many abilities can you pack into an embedding space”. This may appear like a simple restatement of facts, but it is important in that

<sup>4</sup>Sampling  $w_{t+1}$  is equivalent to sampling  $\mathbf{w}_{t+1}$ .

<sup>5</sup>i.e, relative w.r.t. words in the vocabulary

<sup>6</sup>If we consider every point in  $\mathbb{R}^D$  as a valid vector, then the organization of  $\mathbb{S}$  can also be interpreted as a *curvature* or *shape* of  $\mathbb{S}$  since it determines the trajectory of the decoding walk through Embedding Space.

it underscores an important property of neural sequence models that has been overlooked amidst details of architectures and training and inferencing procedures. It also unifies neural sequence models that have a residual stream i.e.,  $f_{\Sigma;\theta}$  could equally be implemented by a RNN, LSTM (Graves, 2014) and the newer post transformer architectures (Gu et al., 2022; Fu et al., 2023; Poli et al., 2023; Sun et al., 2023).

These analyses are equally applicable across modalities and other neural sequence models that are based on embeddings like that have a residual stream.

### 2.2.2 TOKEN NEIGHBORHOODS AND TARGET PATH

In this section we define *neighborhoods* for referencing later. You may skip it for now and come back later when needed. Consider a scenario where the model predicts a sequence  $\langle \mathbf{w}_i \rangle_{T+1}^{T+P}$  of length  $P$  given a context  $\langle \mathbf{w}_i \rangle_1^T$ . Under greedy decoding,  $\langle \mathbf{w}_i \rangle_{T+1}^{T+P}$  consists of words closest to the points  $\langle \mathbf{d}_i \rangle_{T+1}^{T+P}$  on the decoding walk. Therefore if we wanted to produce a target sequence of words - say  $\langle \dot{\mathbf{w}}_i \rangle_{t=T+1}^{T+P}$  - we would need to ensure that every predicted vector  $\mathbf{d}_{\langle \mathbf{w}_i \rangle_1^t}$  fell within a neighborhood  $\mathcal{N}_{\dot{\mathbf{w}}_i}$  of  $\dot{\mathbf{w}}_i$  such that  $\dot{\mathbf{w}}_i$  was its closest token. We shall denote the sequence of these neighborhoods of  $\langle \mathbf{w}_i \rangle_{t_1}^{t_2}$  as  $\mathcal{N}_{\langle \mathbf{w}_i \rangle_{t_1}^{t_2}}$  and we shall say that the decoding walk lies within  $\mathcal{N}_{\langle \mathbf{w}_i \rangle_{t_1}^{t_2}}$  iff  $\mathbf{d}_i \in \mathcal{N}_{\mathbf{w}_i}; \forall i \in [t_1, t_2]$ . Finally, we define  $\mathcal{N}_{\langle \mathbf{w}_i \rangle_{T+1}^{T+P}}$  as the *target path* corresponding to the target sequence  $\langle \mathbf{w}_i \rangle_{T+1}^{T+P}$ .

### 2.3 VECTOR COMPOSITION

$$f_C^l : \mathbb{S}^n \rightarrow \mathbb{S}^n \text{ composition func of encoder layer } l \quad (16)$$

$$\begin{aligned} f_C &: \mathbb{S}^n \rightarrow \mathbb{S}^n \text{ composition func of entire encoder} \\ &= f_C^L \circ f_C^{L-1} \cdots \circ f_C^1 \end{aligned} \quad (17)$$

$$\mathbf{c}_t^l \equiv \text{vector output by encoder layer } l \text{ at position } t$$

$$\mathbf{c}_t \equiv \text{vector output by encoder stack (after final layer norm) at position } t$$

$$\begin{aligned} \langle \mathbf{c}_i^l \rangle_{\langle \mathbf{w}_i \rangle_1^T} &\equiv \text{vector sequence output by encoder layer } l \text{ given input sequence } \langle \mathbf{w}_i \rangle_1^T \\ &= f_C^l \left( \langle \mathbf{c}_i^{l-1} \rangle_{\langle \mathbf{w}_i \rangle_1^T} \right); \langle \mathbf{c}_i^0 \rangle_{\langle \mathbf{w}_i \rangle_1^T} = \langle \mathbf{w}_i \rangle_1^T \\ &= f_C \left( \langle \mathbf{w}_i \rangle_1^T \right) \end{aligned} \quad (18)$$

$$\langle \mathbf{c}_i \rangle_{\langle \mathbf{w}_i \rangle_1^T} \equiv \text{concept vector sequence composed by encoder stack from input } \langle \mathbf{w}_i \rangle_1^T$$

$$f_D^l : \mathbb{S}^n \rightarrow \mathbb{S} \text{ composition func of decoder layer } l \quad (19)$$

$$\begin{aligned} \mathbf{d}_t^l, \mathbf{d}_{\langle \mathbf{w}_i \rangle_1^t}^l &\equiv \text{vector composed by decoder layer } l \text{ at step } t \text{ given input sequence } \langle \mathbf{w}_i \rangle_1^t \\ &= f_D^l \left( \langle \mathbf{c}_i \rangle_{\langle \mathbf{w}_i \rangle_1^T} \sqcup \langle \mathbf{d}_t^{l-1} \rangle_{T+1}^t \right); \sqcup \text{ denotes concatenation} \\ &= f_D^l \left( f_C(\langle \mathbf{w}_i \rangle_1^T) \sqcup \langle \mathbf{d}_{\langle \mathbf{w}_i \rangle_1^t}^{l-1} \rangle_{T+1}^t \right) \end{aligned} \quad (20)$$

$$; T = \text{context length, } \langle \mathbf{d}_t^0 \rangle_{T+1}^t = \langle \mathbf{w}_i \rangle_{T+1}^t, \text{ the decoder input sequence}$$

$$\begin{aligned} f_{\Sigma;\theta} &: \mathbb{V}^n \rightarrow \mathbb{S} \text{ the entire model framed as a composition function} \\ &; \text{ itself composed from } f_D^l \text{ and } f_C \end{aligned} \quad (21)$$

In this section shall decompose  $f_{\Sigma;\theta}$  into layer wise functions and discover that they are composed of two basic types of operations: 1) filtering and 2) aggregation. We shall also examine *attention* in detail, exposing the roles it plays in training and inferencing. We also examine in detail the process of vector composition which we denote the *encoding walk*. Finally we tie everything together into a *mechanics of intelligence*.

Equations 16 through 21 formalize the encoder-decoder Transformer architecture as an algebra. Each layer is cast as a composition function. The layer wise functions  $f_C^l$  and  $f_D^l$  are composed of the *attention layer* and other functions that we simply generalize as *filters*. These are explained next.



Figure 4: (a). Encoding walk of position 223 (input token ‘000’) up a T5 encoder stack. The composed vector stays within the vicinity of the input token. E = token vector, NormSA = layer-norm’d layer input, FinalNorm = stack output. (b) The story is obviously different for decoder stacks where the start token - <pad >- must move into the neighborhood of the predicted token - 1. (c) Similarity map of encoder output for the same few-shot sample as Figure 3. The pattern gets fuzzy here because of combination of context into the token vectors. However the broad pattern persists because the encoder composed vectors generally stay within the neighborhood of the original input token. (d) Abovementioned encoding walks mapped onto a 3D UMAP projection of  $\mathcal{S}$ . Orange dots are input tokens.

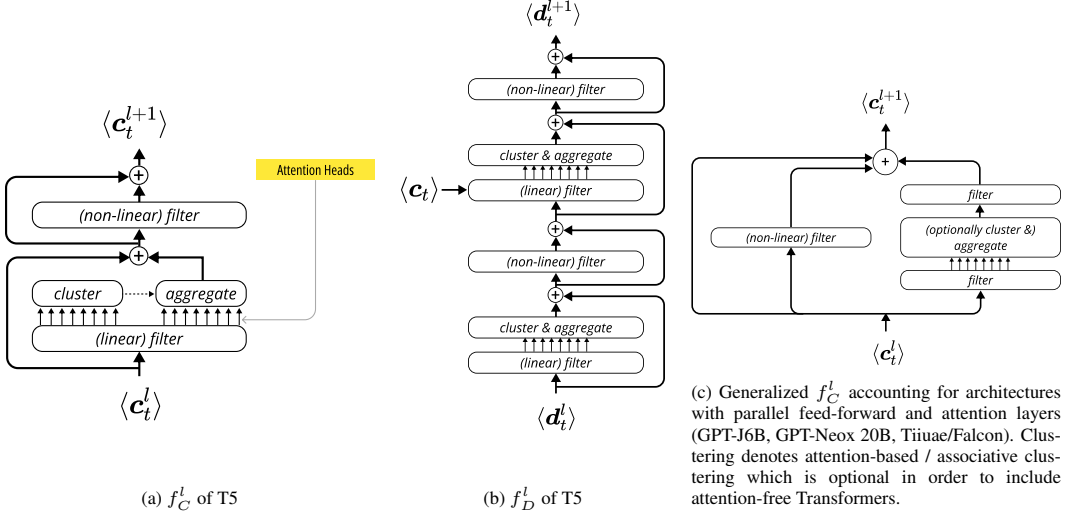


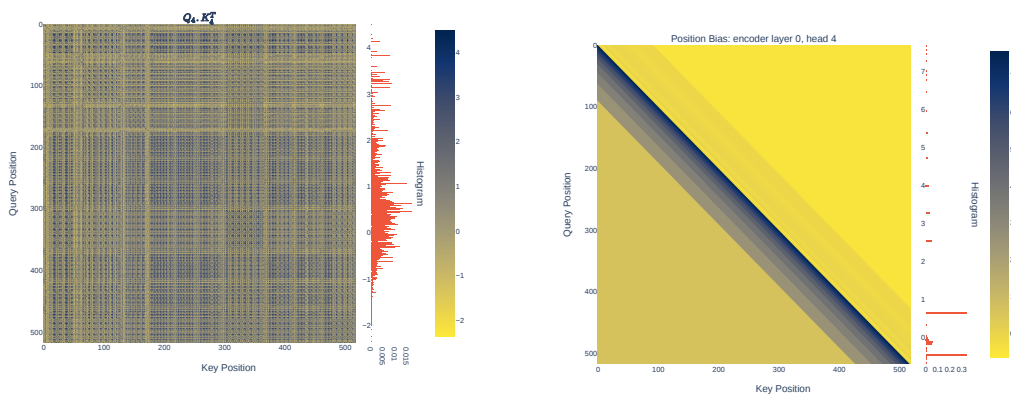
Figure 5: The transformer architecture generalized in terms of filters and soft-clustering operations.

### 2.3.1 FILTERS

The composition functions include point-wise transforms that we call *filters* ( $filter : \mathbb{S} \rightarrow \mathbb{S}$ ). These are (see Figure 1) : 1) Layer norm 2) the key, query, value and output projection matrices  $\mathbf{W}_{k,h}$ ,  $\mathbf{W}_{q,h}$  and  $\mathbf{W}_{v,o,h}$  respectively in the attention layer (sec. A.1) and 3) the nonlinear feed-forward layers. They are *static* functions in the sense that their output only depends on the input vector i.e., there is no interaction between vectors and therefore are these \*not\* composition functions. Self-mapping filters (layer-norm and feed-forward layers and  $\mathbf{W}_{v,o,h}$ ) reshape (rotate) and / or amplify or attenuate (stretch) a vector. The non-linear activation function (RELU or similar) inside the feedforward layer is clearly a filter since it removes (clamps to zero) all values below zero and allows the rest to pass through unchanged. The low-rank matrices  $\mathbf{W}_{k,h}$  and  $\mathbf{W}_{q,h}$  can be viewed as performing the same operations but in a sub-space. Also, since they involve linear transforms, filters cause a mixing of dimensions of  $\mathbb{R}^D$  (also called channel mixing (Sun et al., 2023)) thereby implying that features are redundantly represented across dimensions. To sum it up, filters statically amplify or attenuate features and therefore can be viewed as static feature selectors.

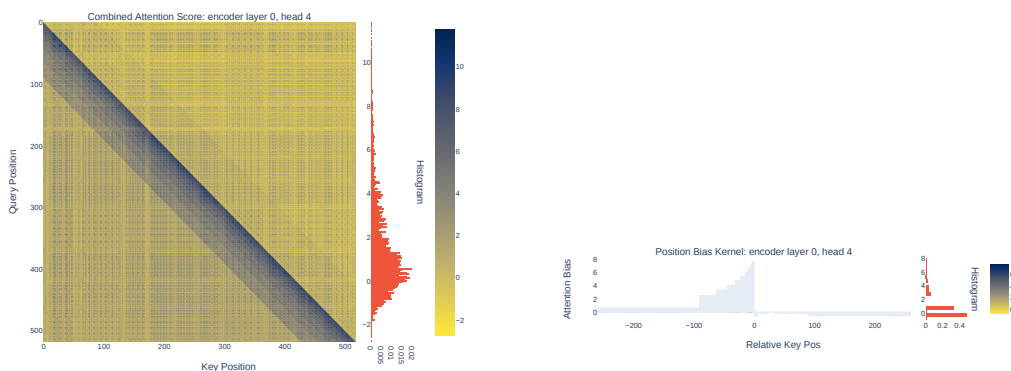
### 2.3.2 ATTENTION LAYER

The *multiheaded attention* operation can be refactored as independent attention paths per attention head by slicing  $\mathbf{W}_o$  into  $H$  slices  $\mathbf{W}_{o,h}$  one per head, who's outputs are summed (see section A.1 for the derivations). Each head therefore independently *aggregates context* around a query position, with the (filtered) context vectors being weighted by their normalized similarity (softmaxed inner product) to the (filtered) query and by their position in the sequence (via relative position biases). A quick note regarding nomenclature: while the inner product is carried out on vectors filtered by key and query matrices  $\mathbf{W}_{k,h}$  and  $\mathbf{W}_{q,h}$  resp. and the context vectors are filtered by the value-output matrix  $\mathbf{W}_{v,o,h}$  before summation, the filtrations amount to feature selection as explained in section 2.3.1 and therefore the vectors are still identified as the 'same' vector, just filtered. Hence when we say 'query vector' we are referring to the vector at the query position, filtered or unfiltered depending on the context. Coming back, given the analyses so far, attention can be generalized into the following two steps. 1) **Cluster**: compute a *soft-cluster* for each query vector  $w_t$ ; use attention weights as the degree of cluster membership i.e., "gather similar stuff from selected locations" and 2) **Aggregate**: aggregate the cluster by membership score i.e., compute the soft cluster centroid. This amounts to the following sequence of operations:  $filter \rightarrow cluster \& aggregate \rightarrow filter$ . The two linear filters can be merged together (section A.1) to yield  $filter \rightarrow cluster \& aggregate$ . Adding feed-forward layers and residual connections into the picture we can generalize the Transformer architecture as shown in (Figure 5).



(a) Attention Scores: Inner product of query and key vectors without bias

(b) Position biases with negative self bias (-0.66)



(c) Attention weights before softmax = Attention scores + position biases. Position bias significantly influences attention scores.

(d) Position kernel corresponding to 6b and 6c. Position zero (self) is in the middle. Amplifies a band on the left side. Right hand side positions including the middle (self) are suppressed.

Figure 6: Pretrained Flan-T5-XL encoder attention layer activation maps.

**Weighted Bag of Words** Note that while relative positions influence the aggregation scores (i.e. attention weights) they are not directly stored in the aggregated vector. Position biases can only influence it by changing the composition of the cluster. In the T5 architecture, each head learns a distinct shape of relative position bias which influences the attention weight distribution over the sequence. We call the relative position biases the *position kernel* since they are similar to a 1D convolution kernel (Figs. 7 and 9). In T5-small and Flan-T5-XL models, we found that the magnitudes of the biases are large enough to significantly influence attention weights (Figs. 6 and 8). After aggregation however, the sequence information is lost and hence the aggregation procedure can be thought of as a weighted bag of words. We emphasize that THERE IS NO OTHER MECHANISM, BESIDES POSITION BIASES, IN TRANSFORMER ARCHITECTURES TO INCORPORATE SEQUENCE INFORMATION.

**Negative Self Bias** While we haven't yet performed an exhaustive survey of learnt position biases across all popular models, analyses of T5 models gives us confidence that position biases play a significant role in vector composition for the T5 and perhaps for other architecture flavors as well. In particular about 80% of the position kernels (one per head) in the T5-Small and Flan-T5-XL encoders significantly attenuate the query's own attention weight (Fig. 7). In its decoder stack we found about 30% self-attention heads that amplify far away locations (Fig. 9). In both these cases, context is aggregated primarily from foreign locations i.e. locations excluding the query itself, thereby suppressing the its membership in its own cluster. This also happens in cross-attention where the aggregated context does not include the query at all. We call this phenomenon *negative self-bias*. This amounts to a copy-in from foreign locations. In our framing however, instead of

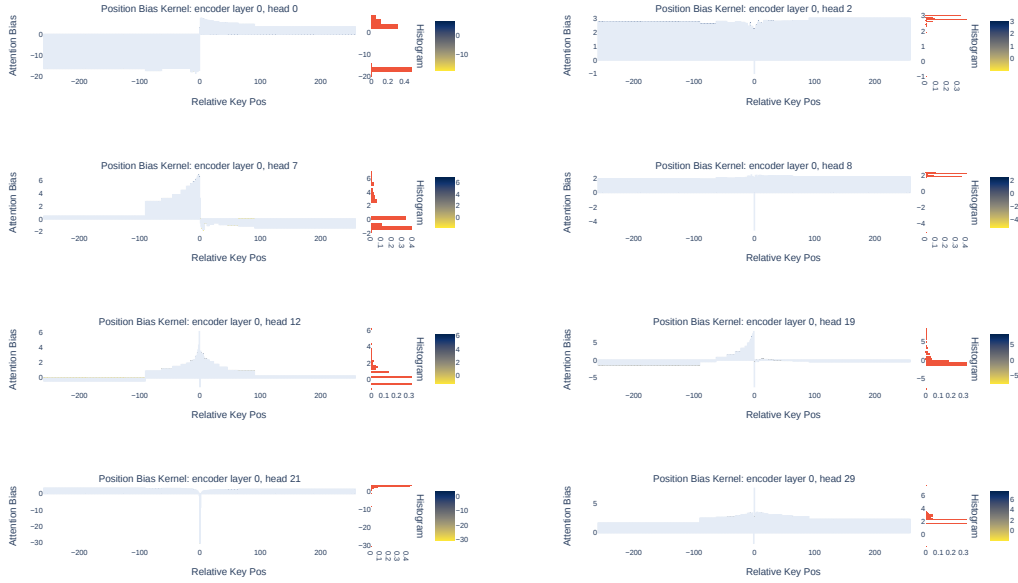
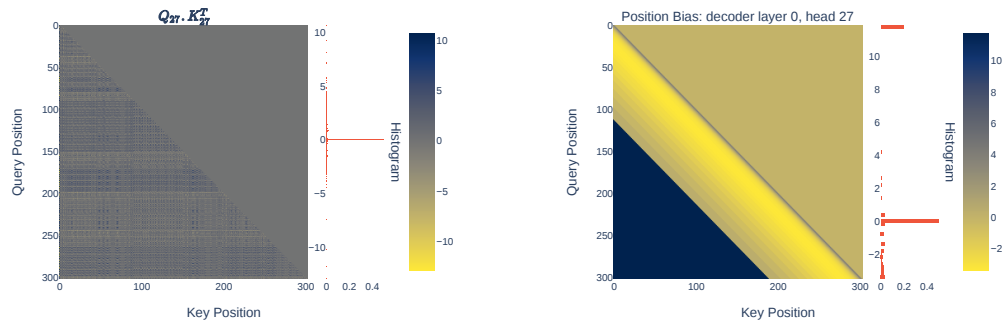


Figure 7: Some position kernels of a pretrained Flan-T5-XL encoder.

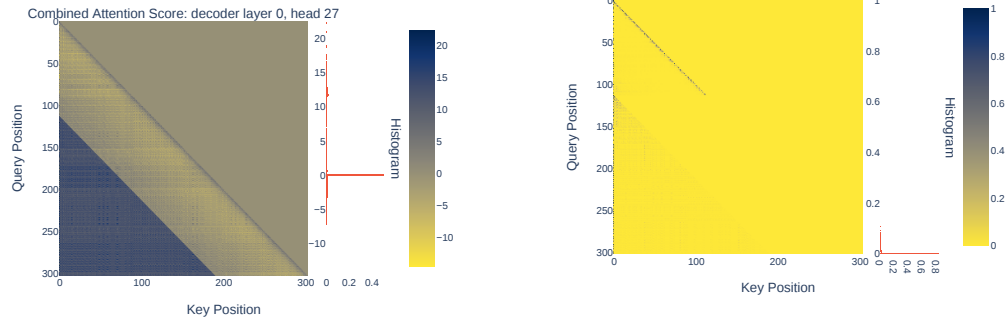
saying that context has been copied into the query location, we say that the query vector moves into the center (i.e., centroid) of the context cluster. As a corollary, if this context was obtained entirely from foreign locations, then the centroid point could be significantly far from the query. Negative self-bias goes counter to popular intuition that position bias must be greatest at position 0 (query position) and then decrease gradually from there. However, negative self-bias is necessary to allow the query vector to escape its “gravitational pull of self association” i.e. the degenerate scenario where the query token is predicted over and over because it is most similar to itself (Holtzman et al., 2020). Without negative self-bias, the query vector would dominate its cluster since it is likely to have the highest inner-product with itself. The subsequent summation with the residual vector - an unfiltered version of itself - would further exacerbate this situation. As discussed later in section 2.3.3, a query vector must escape its neighborhood - at least in the greedy or beam-search decoding regimes and when the input/output embedding matrices are tied (which is by far the majority case) - in order for the next token to be predicted successfully.

**Similarity, Co-Occurrence and Angular Distance** *Cluster & aggregate* is the only operation that involves interaction amongst vectors (also called *data dependence* in literature). As analyzed, the effect of this operation is to aggregate features from across the context. Consequentially, the composite decoding vector  $d_t$  ultimately produced at the top of the stack, contains aggregated features from the context  $\langle w_i \rangle_1^t$  which the denoising training objective (e.g. MLM or LM) nudges to come closer to the target token vector  $w_{t+1}$ . This effect is same as that explicitly sought by distributed word representation models such as Word2Vec (Mikolov et al., 2013a) except that aggregation of context here is performed implicitly (by the attention layer) and that the aggregation weights are influenced by vector similarity. This will cause filtered vectors and consequently token embeddings that co-occur frequently to come closer together in the Embedding Space thereby further increasing their similarity score and so on until either an equilibrium is reached or training stops. It follows therefore, that similarity in  $\mathbb{S}$  is a proxy for co-occurrence / association. Notably, denoising training objectives will also cause context representations  $d_{(\langle w_i \rangle_1^t)}$  to come closer to the target co-occurring words  $w_{t+1}$ . Also, as stated before, since the vector magnitudes are bounded (due to layer-norm), similarity implies angular proximity too. Therefore one would expect highly co-occurring tokens to cluster together angle-wise in Embedding Space. Empirically we observe all of these effects. In figures 3 we see closely associated tokens such as numbers and brackets exhibit high similarity scores. Broadly co-occurring tokens such as section separators of formatted samples exhibit low similarity across the board. The effects are even more pronounced when the vectors are normal-



(a) Attention Scores: Inner product of query and key vectors without position bias

(b) Position biases with positive self bias (2.12). Position kernel is in Fig. 9



(c) Attention weights before softmax = attention scores + position biases. Position bias significantly influences attention scores.

(d) Attention weights (after softmax). Self bias (dark diagonal line) quickly dissipates as soon as the impact of foreign context imposed by position bias (bottom left dark triangle in Fig. 8c) kicks in.

Figure 8: Pretrained Flan-T5-XL decoder attention layer activation maps.

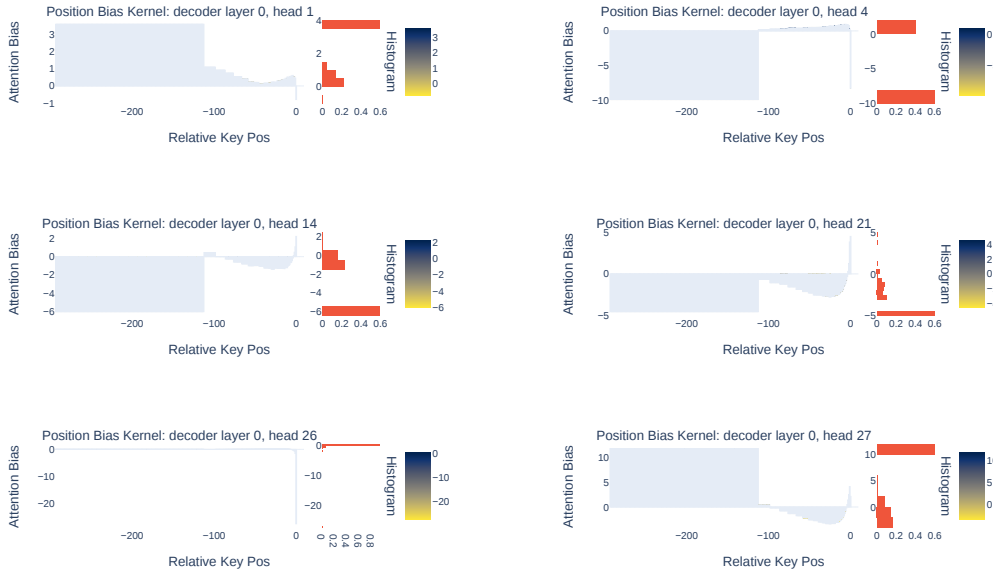


Figure 9: Some position kernels of a pretrained Flan-T5-XL decoder. In the bottom right is position kernel for head 27, corresponding to 8b and 8c. Position zero (self) is the right most position. Amplifies the far left positions and self. An intermediate band is suppressed.

ized by layer-norm or L2-norm (i.e., when comparing via cosine-similarity). More such patterns are shown in the appendix for pretrained flan-t5-large (encoder-decoder) (Fig. 11) and falcon-7b (decoder only) (Penedo et al., 2023) (Fig. 12) models. Thus a three way correspondence between Similarity (inner-product), association (co-occurrence) and angular proximity (cosine similarity) is established. **This role that attention plays in co-locating co-occurring token embeddings during training has been largely overlooked so far.**

**Associative vs Non-Associative Aggregation** In a nutshell, the attention layer implements position biased associative aggregation. The association aspect seems to be important since attention-free models i.e. those with non-associative aggregation i.e., attention-free architectures (Hochreiter & Schmidhuber, 1997a; Gu et al., 2022; Fu et al., 2023; Poli et al., 2023) do not perform as well as Transformers (Vardasbi et al., 2023). Please note though that they can still organize  $\mathbb{S}$  associatively due to the stochastic nature of training. These models are quickly catching up, therefore the role of similarity in attention may not be necessary after all.

### 2.3.3 THE ENCODING WALK

If you follow the path of a vector  $e_t^l$  as it moves up a encoder or decoder stack (henceforth *encoding vector*), it starts off as  $w_t$  in layer 0 and, with every layer it traverses upwards, it “attracts” and aggregates “similar context from selected locations” until it finally emerges at the top as either  $c_t$  or  $d_t$ . Note that with every such step the encoding vector itself gets pulled in the direction of the context it aggregated, which in turn influences what it attracts the next time around. We call this traversal the *encoding walk* (fig. 4) and it is steered by 1) the vectors present in the context, 2) “the pull of association” between them i.e. the inner-product of their filtered versions, 3) the sequence-pattern, indirectly enforced via relative position-biases and 4) the static filters  $W_{v,o,h}$  that ultimately select the features to aggregate. Since  $W_{v,o,h}$  are fixed, they get marginalized w.r.t. dynamic behaviour, leaving only the first three factors to govern in-context learning. Further, if the feedforward layers had the RELU function - which can be viewed as a multiplication with a diagonal matrix with ones and zeros - then the entire encoding walk becomes a linear transform. This implies that the range of the encoding walk is limited to the linear span of the token vectors of its context - i.e., it is entirely bounded by the context. In particular all encoding walks are bounded by the linear span

of  $\mathbb{V}$ . However, this is not a limiting factor if  $\mathbb{V}$  was (roughly) uniformly distributed all around a disk, which could very well be the case here since we’ve seen empirically that mutual distances are bounded (fig. 2).

In the decoder stack, each such traversal up the stack constitutes one step of the decoding walk, culminating in the final aggregated vector  $\mathbf{d}_t$ ; and the next predicted token  $w_{t+1}$  is picked from it’s neighborhood. The LM training objective in turn forces this neighborhood to be populated with tokens that are correlated (in expectation) with the aggregated context. Putting this together with the abovementioned three factors of in-context learning, it follows that the decoding walk - a dynamic process - is ultimately governed by the joint co-occurrence of feature (filtered vector) sequences. This aligns very well with the task of pattern recognition because a pattern can be defined as a sequence of features. In conclusion, all the intelligent behavior learnt by the Transformer is determined by the joint co-occurrence of feature sequences presented to it during training. Since  $\mathbb{S}$  is a continuous space, the model generalizes at inference time by walking on low-entropy paths through  $\mathbb{S}^7$ , all decoding walks being bounded by the linear span of  $\mathbb{V}$  which is possibly organized as a disk.

**Encoder vs Decoder Walks** On the mechanical side of things, we observe empirically that in the encoder stack  $c_t^L$  stays within vicinity of  $w_t$  i.e.  $\mathcal{N}_{w_t}$ , which is expected since the target token is the input itself (Fig. 4a). In the decoder stack where the output un-embedding matrix is tied to the input embedding matrix however, the output vector strays away from  $w_t$  (Fig. 4b) since its training objective is to predict the next token, not the input token. However, for a model like T5 which has both an encoder and a decoder, it is instructive to examine how the stacks behave differently. The behaviour of the encoder stack is understandable since the “pull of self association” of the primary vector  $w_t$  is expected to be strong given that it is highly correlated with itself (because it’s mutual angle with itself is zero) and that residual connections should further help keep it in it’s own neighborhood  $\mathcal{N}_{w_t}$ . In the decoder stack however,  $w_t$  must move out of it’s own neighborhood  $\mathcal{N}_{w_t}$  and into the “foreign” neighborhood  $\mathcal{N}_{w_{t+1}}$ . In order to do this it would need to overcome the strong “self-association pull” by aggregating sufficient amount of foreign context as it moves up through the layers. The only way that can happen is if the cumulative mass of attention placed on foreign locations i.e. on vectors other than the query, was much higher than in the encoder stack. This could happen via the context pulled in from the encoder by cross-attention in addition to negative self bias exerted by position biases. We see this happening in Fig. 8c where the self bias (dark diagonal) dissipates the moment the far left context kicks in. For decoder-only architectures<sup>8</sup> however, there is no cross-attention and therefore  $w_t$  must overcome self-association pull purely through context aggregated by self-attention. Negative self-bias exerted by position biases as discussed in section 2.3.2 is the only mechanism we have found that can accomplish this in decoder-only models. However, the GPT series of models only has global attention which, being inserted at the input layer would quickly dissipate after aggregation in layer 1. So, how negative self-bias is exerted in those models is a mystery to us. Perhaps an interplay between filters and the organization of  $\mathbb{S}$ ? Plus the fact that generative decoding is performed via. stochastic sampling (Holtzman et al., 2020) not greedy decoding (which is known to cause degenerate repetition), relaxes this constraint? We haven’t done enough investigation into this topic to have the answers. Specifically, the relative impact of the following four factors across various model flavors needs further investigation: 1) vector similarity, 2) position biases 3) filters and 4) decoding method.

### 3 THE MECHANICS OF INTELLIGENCE

The above discussion highlights a couple of points: 1) *Cluster & aggregate* is the only operation that involves interaction between positions and that happens via position-biased associative aggregation. Without it the Transformer would degrade to a point wise FF stack with no interaction between positions, completely incapable of recognizing patterns in the context<sup>9</sup>. 2) Aggregation on the other hand, results in loss of explicit sequence information as explained in section 2.3.2. Hence, unlike a CNN which is imbued with spatial kernels, there is no mechanism in the transformer to even learn static sequential patterns, let alone dynamically as it may appear it does when “learning

<sup>7</sup>Because the decoding sampling favors higher-probability tokens.

<sup>8</sup>... where the in/out embedding matrices are tied, which is the majority case

<sup>9</sup>Unless the training objective was altered to cause such interaction.

from few-shots”. Intelligent behaviour i.e., a desirable decoding walk therefore occurs only due to 1) composition of context into a representation vector  $d_{\langle w_i \rangle_1^t}$  eschewing explicit sequence information and 2) proximity of this representation with co-occurring token representations  $w_{t+1}$  such that  $d_{\langle w_i \rangle_1^t} \in \mathcal{N}_{w_{t+1}}$ . These two conditions are imbued in **the organization of Embedding Space**.

Take for e.g. the patterns observed in figures 3, 4c<sup>10</sup> which clearly demarcate 9 segments of the few-shot input: one question, one rubric, six examples and one query sample. Each of the segments is of varying length, which may lead one to believe that the model ‘recognizes’ the pattern and therefore is able to complete it. However a much simpler and mechanical explanation is that the segment markers are broadly correlated with all tokens and therefore have weak similarity with them resulting in the light colored bands. Next, the answers themselves are made up of very similar tokens - brackets and numbers, which being highly correlated cause the appearance of dark square patterns.

**Intelligence is a System Level Property** It does seem after all that the generative Transformer is ‘merely’ a token prediction engine, a mere “stochastic parrot”. However, there is no denying the fact that Transformer based Large Foundation Models exhibit remarkably intelligent behaviours. Therefore it does seem that intelligent behaviour in a Transformer - or any embeddings space based neural sequence model - emerges at a system level, rather than the mechanical level. We have shown that the system in question here is the Embedding Space and its *organization* as defined here. Hence we believe that more research needs to happen at the intersection of embedding space geometries and cognitive science.

**It’s always hallucinating** Decoding walks are random walks regardless of whether the generated sequence may depict fact or fiction. Both facts and fiction are low-entropy paths through  $\mathbb{S}$ .

## 4 RELATED WORK

This work details and expands our previous work “The Transformer Algorithm” (Singh, 2021) where we introduced the embedding space centric framework. Around the same time Elhage et al. (2021) and Olsson et al. (2022) introduced a mathematical framework which included the notion of a “residual stream”, a working memory / bandwidth from which attention heads read and write into, thereby implying the existence of a common vector space, same as ours. However, they view it’s purpose as a communication channel between layers and as temporary storage of information as opposed to our viewpoint wherein it plays a much more central and encompassing role: an abstract space that not only embodies information but also intelligence and skill as low-entropy paths. In their formulation the job of attention heads is to move information between positions, whereas in our theory heads perform associative aggregation - the mechanics that give rise to the “forces of association” that shape encoding and decoding walks through Embedding Space. They further go on to study synthetically constructed 1-2 layer decoder-only, attention-only, linear models (i.e with the feed-forward and layer-norm layers removed) attempting to discover patterns that can be hopefully generalized to full Transformers. In these synthetic models they explore “induction heads” as the method of in-context learning - an isolated pair of attention-heads across layers that work together to copy in the token following a previous occurrence of the query. However induction heads do not explain how the model generates non-repetitive text. Also, the behaviour of an isolated circuit may easily be overshadowed by other concurrent circuits. While this approach of isolating circuits is certainly a useful and necessary one, this work takes a more system-level approach attempting to answer the same questions via the encoding and decoding walk analyses. Geva et al. (2022); Dar et al. (2022) espouse a vocabulary centric viewpoint. They view the token embedding vectors as an overcomplete basis for representing activation and weights matrices and apply it for steering inference and transferring knowledge across models. Our framework on the other hand just reuses the  $d_{model}$  dimensions of the token embeddings as the basis of the vector space and our objective is to explain intelligent behavior in general. Dai et al. (2023) and von Oswald et al. (2023) propose that self-attention equations when simplified to linear transforms only, under autoregressive decoding, can be reinterpreted as performing gradient descent across sequence positions. While this is a great orthogonal viewpoint - albeit it applies only to linear attention - it is still unclear what loss func-

<sup>10</sup>More in the appendix (figs. 11 & 12)

tion is being optimized here. Also, training of token vectors  $\mathbb{V}$  is absent from this picture. While the approach of carefully studying the mathematics of small linear-models is certainly a useful and necessary one, we chose to study and experiment on real-world models - about 15 - ranging from 70 million to 13 billion parameters in size.

## 5 EXPERIMENTS

Since the objective of this work is to link the underlying mechanics of sequence models with their high level semantic behaviors, we tested a semantic interpretation of embedding vectors.

### 5.1 SEMANTIC SPACE THEORY

In recent literature embeddings are implicitly viewed as embodying meaning. This notion is especially prevalent in multimodal models (Li et al., 2016; Radford et al., 2021; Lu et al., 2022; Kerr et al., 2023; Reed et al., 2022; Girdhar et al., 2023) where different modalities share a common embedding space. This is also the case with multilingual language models or machine translation sequence to sequence models wherein the same embedding space is shared by different languages. Formalizing this intuition, we redefine *embedding vector* (both  $\mathbf{w}$  and  $e_{\langle \mathbf{w}_i \rangle}$ ) to *concept vector* and *embedding space* to *semantic space*. Semantic space is populated with concepts; coherent / incoherent, complete / incomplete and often themselves composed from other concepts in a part-whole hierarchy. Concepts serve as a building blocks of the semantic understanding exhibited by the model. Zero-shot instructions, few-shot prompts, chat history as well as the model’s CoT reasoning, plans, observations and reflections are all (composite) concepts. Composite concepts are first class citizens of the *semantic space*  $\mathbb{S}$  alongside token-vectors. We test the following implied properties of this theory:

1. Property 1: Like in natural language, concepts may be recursively composed from other sub-concepts in a part-whole hierarchy. In other words, the composition function (sec 2.3) is summative and associative. Elhage et al. (2021) and Geva et al. (2022) also posit the summative nature of embedding vectors.
  - (a) Therefore it should be possible to predict tokens by replacing the input context’s token sequence with a sequence of pre-aggregated concepts i.e.,  $f_{\Sigma}(\langle \mathbf{w}_i \rangle_{T_0}^{T_n}) = f_{\Sigma}(\langle f_{\oplus}(\langle \mathbf{w}_i \rangle_{T_1}^{T_2}) \cdots f_{\oplus}(\langle \mathbf{w}_i \rangle_{T_{n-1}}^{T_n}) \rangle)$  where  $f_{\oplus}(\langle \mathbf{w}_i \rangle_{T_i}^{T_{i+1}}) \in \mathbb{R}^D$  is the aggregated concept vector of the partial sequence  $\langle \mathbf{w}_i \rangle_{T_i}^{T_{i+1}}$ .  $f_{\oplus} : \mathbb{R}^{n \times D} \rightarrow \mathbb{R}^D$ , is the concept composition function, itself composed from  $f_C$  for encoder-decoder models and from  $f_{\Sigma}$  for decoder-only models.
2. Property 2: Since composite concepts are first-class citizens of  $\mathbb{S}$ , they should organize associatively in  $\mathbb{S}$  just like tokens (sec. 2.3.2).
  - (a) Therefore, it should be possible to perform a decoding walk of composite concepts i.e., predict the next concept  $f_{\oplus}(\langle \mathbf{w}_i \rangle_{T_n}^{T_{n+1}})$  given a sequence of concepts  $\langle f_{\oplus}(\langle \mathbf{w}_i \rangle_{T_1}^{T_2}) \cdots f_{\oplus}(\langle \mathbf{w}_i \rangle_{T_{n-1}}^{T_n}) \rangle$ .

**Hierarchical Concept Composition** We tested these properties on 14 pretrained models on the Hellaswag benchmark (Zellers et al., 2019). The Hellaswag task is to choose one of 4 completion sentences given a few-shot context comprising of 0 or more example passages followed by a query passage. We tested both zero and 5-shot versions of this test with the following segmentation schemes: 1) each sentence is a segment (*segment\_sentences*), 2) the context and completion parts of each example are segments (*segment\_each\_example*), 3) each zero/few-shot example is one segment (*concat\_each\_example*) and 4) all examples of the context concatenated together form one (and only one) segment (*concat\_all\_examples*). For comparing across models, we settled on a pyramidal aggregation scheme for  $f_{\oplus}$  wherein we start with contextualized token vectors  $e_t$  of a segment and aggregate them into a single segment embedding vector. This is optionally followed by aggregation of segment vectors within an example and then optionally the aggregation of all example vectors. The argument here is that a semantically sound pyramidal partitioning i.e. sentences  $\rightarrow$  sections  $\rightarrow$

examples  $\rightarrow$  full-context, should yield the best results from a model that understands semantics of language and it’s part-whole hierarchy. For encoder-decoder models,  $e_t = c_t$  and for decoder-only models,  $e_t = d_t$ . The token-aggregation function for encoder-decoder models was (element-wise) *mean*, while for decoder-only models we used a weighted mean (denoted *wlmean*) where the  $i^{th}$  vector in a sequence of  $N$  vectors is weighted by  $i/N$ . Segment and example vectors were aggregated via *mean* if applicable. We shall call this the *standard concept composition scheme*. For select models, we also tested several variations of this scheme, as explained later.

### 5.1.1 TEST 1: TOKEN GENERATION CONDITIONED ON AGGREGATED CONCEPTS

To test property 1, we compute segment vectors as described above, yielding a sequence of vectors representing the context. The token vectors of a completion sentence (one of the 4 choices) are then concatenated to it and the result fed to the model as input embeddings. Joint probability of the completion sentence is then obtained from the model’s output probabilities and used to pick the winning choice. Except for the preaggregation of context segments, this is the standard procedure used to evaluate language models against Hellaswag. We modified the Language Evaluation Harness (Gao et al., 2021) for this purpose. Our code is available as open source<sup>11</sup>.

Figure 10a shows the scores of 11 decoder-only and 3 encoder-decoder models. All of these models were obtained from the Huggingface transformers library (Wolf et al., 2020). The scores shown are normalized by the model’s baseline hellaswag score computed as usual with the full token-sequence as input. If property 1 holds and if the composition scheme was correct, then we expect this method to do as well as the baseline i.e. a normalized score = 1.0. However as we see in Fig. 10a, none of the models achieve the baseline.

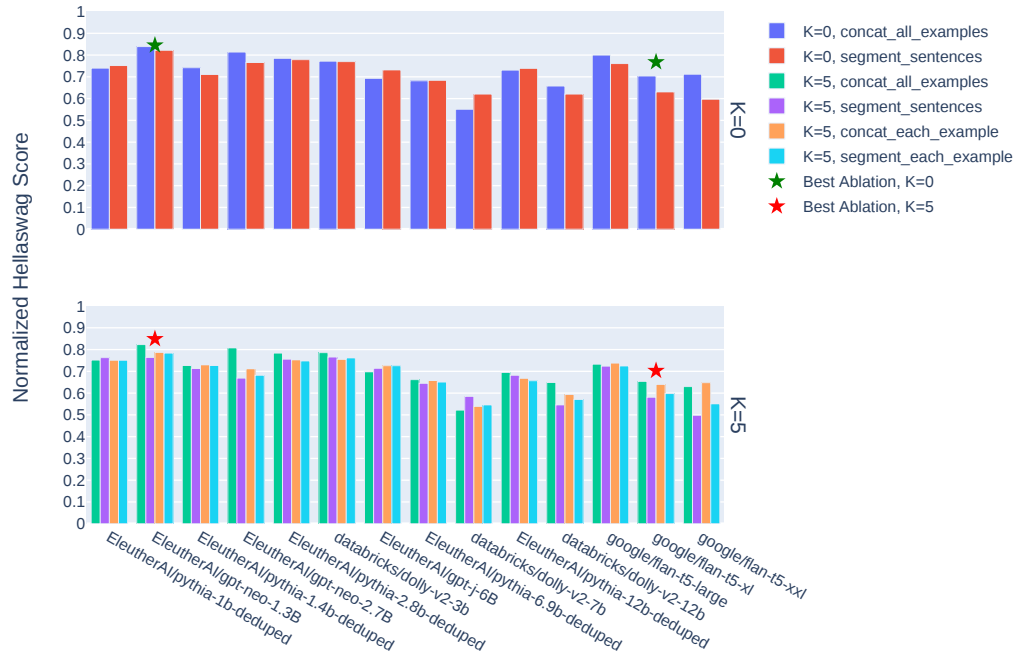
This could mean that either the hypotheses are not true, are partially true and/or the standard composition scheme was incorrect. For e.g. one could argue that the top-layer of the stack is perhaps not the best place to pick token embeddings for all models - that perhaps it should be an intermediate layer for decoder-only models because since it has only one Transformer stack, that may have partitioned itself into an encoder stack followed by a decoder, thereby mimicking an encoder-decoder model. Or that perhaps the aggregation function  $f_{\oplus}$  should be machine-learnt. Therefore we tried several versions of the segmentation and aggregation functions and attempted to find the best combination i.e., the best concept composition scheme. However, the best performing scheme turned out to be unique per model, much like a machine-learnt function would have. Therefore we consider it a proxy for the ideal machine-learnt scheme and consequently rely on that score as a true test score. A few top performing schemes for gpt-neo-1.3B (decoder-only) and flan-t5-xl (encoder-decoder) models are reported in section A.3 and all other results are available in our code repository (about 1200) scores of the top performing schemes are shown with a  $\star$  marker.

Decoder-only models generally performed better than encoder-decoder models of the same size in this test, the best scores being 83.9% and 82.3% for zero and 5-shot respectively for gpt-neo-1.3b. Its best composition scheme scores (marked with a  $\star$ ) were 84.5% and 84.9% respectively. Encoder-decoder model results are generally lower with the best value being around 80% for zero-shot and 73.8% for 5-shot for flan-t5-large. Since the scores are all under 100%, semantic space theory is clearly not proven. However, values close to 85% despite using simple hand-crafted composition schemes do indicate at least partial support for the theory.

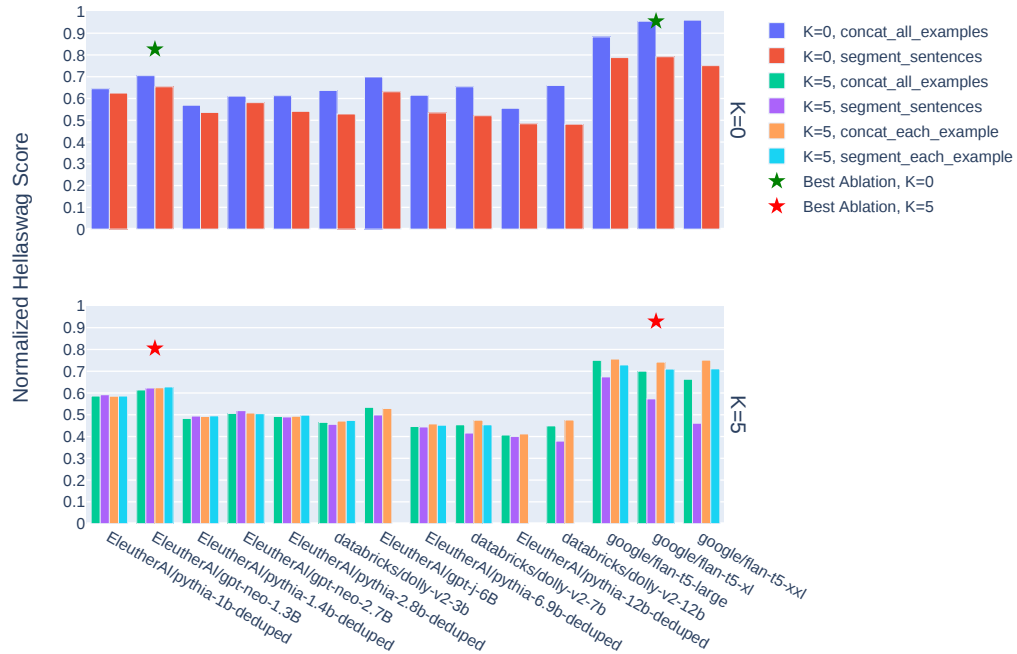
### 5.1.2 TEST 2: CONCEPT SIMILARITY

Here we test property 2 of the semantic space theory. We embed the Hellaswag context into a single vector using the pyramidal aggregation scheme described earlier and do the same for each choice sequence considered as exactly one segment. Then we compare the context and completions via dot-product and pick the winning choice i.e., we predict  $f_{\oplus}(\langle w_i \rangle_{T_n}^{T_{n+1}})$  given  $f_{\oplus}(\langle w_i \rangle_{T_1}^{T_n})$ . This procedure is reminiscent of asymmetric semantic search (Reimers & Gurevych, 2019) commonly employed for retrieval augmented generation (Lewis et al., 2021). In those cases however, the embedding models are fine-tuned or trained for embedding passages but we are using vanilla generative models instead. As with test 1, we also test various permutations of composition schemes for gpt-neo-1.3B and flan-t5-xl models amounting to a total of over 6000, all of which are available in our code repository. This includes schemes that produce a concept vector sequence instead of a single

<sup>11</sup>Source code for Experiments: [https://github.com/Turnitin-AI-Research/lm\\_eval\\_harness](https://github.com/Turnitin-AI-Research/lm_eval_harness)



(a) Pyramidal Generation: Test 1



(b) Concept Similarity: Test 2

Figure 10: Test 1& 2 results: a) Pyramidal generation and b) Concept similarity test.

vector for the context. In such cases each vector of the sequence is compared with the choice vector and the best match is used for picking the choice.

Fig. 10b shows normalized Hellaswag scores of this test. One thing that pops up clearly is that all three encoder-decoder models perform much better than decoder-only models, achieving up to 96% score. This is perhaps since they have a separate encoder stack which we used to encode the sequences. A 95+% normalized score definitely lends support to the semantic space theory, given that we are using a very simple  $f_{\oplus}$  operator. Decoder-only models do much worse, with the best composition scheme on the decoder-only side (for gpt-neo-1.3b) being 82.6% and 80.5% for zero-shot and 5-shot respectively. This could be because lack of an encoder stack makes finding the ideal  $f_{\oplus}$  harder. That said, scores  $> 80\%$  are not insignificant.

### 5.1.3 SUMMARY OF RESULTS

Although the results are not decisively in favor of the semantic space theory, they are high enough to be taken seriously. In particular 95+% scores of the encoder-decoder models on test 2 are encouraging. That said, the scores are largely less than 100% indicating that perhaps the concept-space theory only partly explains the dynamics of Transformers and that Transformers are largely token-sequence  $\rightarrow$  token mappers rather than concept  $\rightarrow$  concept mappers.

## 6 CONCLUSION

Through analyses we’ve shown that the dynamics of generative Transformers can be viewed as a random walk in Embedding Space  $\mathbb{S}$  steered by the proximity of the context sequence representation to tokens in  $\mathbb{V}^{12}$ . Therefore the intelligence exhibited by these models is embodied in the organization of the  $\mathbb{S}$  which, in turn is determined by the vector composition function  $f_{\Sigma}$  and the organization of  $\mathbb{V}$ . Generated sequences are low-entropy paths in  $\mathbb{S}$ . Token vectors organize in  $\mathbb{S}$  per mutual association / co-occurrence and we’ve also seen evidence of similar organization amongst concept vectors. Context aggregation (in the attention layer), being the only *data-dependent* operation, is responsible for organizing composite vectors in  $\mathbb{S}$  (via the encoding walk), which in turn determines decoding walks and the ensuing intelligent behavior (or intelligence). Intelligence and skills exhibited by these models is a system phenomenon emerging from the joint co-occurrence of sequences. It should therefore be studied from a systems point of view rather than a reductionist one. Transformers employ position-biased associative aggregation (attention layer) whereas attention-free architectures only employ position-biased aggregation; it remains to be studied how important associative aggregation is to the emergence of intelligence. These analyses are equally applicable across modalities and other neural sequence models that have a residual stream e.g., generative RNNs, LSTMs (Graves, 2014) and the newer post transformer architectures (Gu et al., 2022; Fu et al., 2023; Poli et al., 2023; Sun et al., 2023). Thereby we arrive at a generalized architecture that’s based on two very simple primitives - filtering and aggregation. We hope that these insights will guide the design of better neural sequence models, spur new research at the intersection of embedding space geometries and cognitive science, and ultimately lead to a deeper understanding of intelligence.

## ACKNOWLEDGMENTS

We’d like to express our heartfelt appreciation to Dr. Eric Wang for his constant support of this project and commitment to research and innovation.

## REFERENCES

Jean-Baptiste Alayrac, Jeff Donahue, Pauline Luc, Antoine Miech, Iain Barr, Yana Hasson, Karel Lenc, Arthur Mensch, Katie Millican, Malcolm Reynolds, Roman Ring, Eliza Rutherford, Serkan Cabi, Tengda Han, Zhitao Gong, Sina Samangooei, Marianne Monteiro, Jacob Menick, Sebastian Borgeaud, Andrew Brock, Aida Nematzadeh, Sahand Sharifzadeh, Mikolaj Binkowski, Ricardo

<sup>12</sup>The arguments in this paper do not change materially when input and output embedding vectors are not tied.

- Barreira, Oriol Vinyals, Andrew Zisserman, and Karen Simonyan. Flamingo: a visual language model for few-shot learning, 2022.
- Jimmy Ba, Volodymyr Mnih, and Koray Kavukcuoglu. Multiple object recognition with visual attention. *CoRR*, abs/1412.7755, 2014.
- Dzmitry Bahdanau, Kyunghyun Cho, and Yoshua Bengio. Neural machine translation by jointly learning to align and translate, 2014. URL <https://arxiv.org/abs/1409.0473>.
- Yoshua Bengio, Réjean Ducharme, Pascal Vincent, and Christian Janvin. A neural probabilistic language model. *J. Mach. Learn. Res.*, 3(null):1137–1155, mar 2003. ISSN 1532-4435.
- Tom B. Brown, Benjamin Mann, Nick Ryder, Melanie Subbiah, Jared Kaplan, Prafulla Dhariwal, Arvind Neelakantan, Pranav Shyam, Girish Sastry, Amanda Askell, Sandhini Agarwal, Ariel Herbert-Voss, Gretchen Krueger, Tom Henighan, Rewon Child, Aditya Ramesh, Daniel M. Ziegler, Jeffrey Wu, Clemens Winter, Christopher Hesse, Mark Chen, Eric Sigler, Matusz Litwin, Scott Gray, Benjamin Chess, Jack Clark, Christopher Berner, Sam McCandlish, Alec Radford, Ilya Sutskever, and Dario Amodei. Language models are few-shot learners. *CoRR*, abs/2005.14165, 2020.
- Sébastien Bubeck, Varun Chandrasekaran, Ronen Eldan, Johannes Gehrke, Eric Horvitz, Ece Kamar, Peter Lee, Yin Tat Lee, Yuanzhi Li, Scott Lundberg, Harsha Nori, Hamid Palangi, Marco Tulio Ribeiro, and Yi Zhang. Sparks of artificial general intelligence: Early experiments with gpt-4, 2023.
- Mark Chen, Alec Radford, Rewon Child, Jeffrey Wu, Heewoo Jun, David Luan, and Ilya Sutskever. Generative pretraining from pixels. In Hal Daumé III and Aarti Singh (eds.), *Proceedings of the 37th International Conference on Machine Learning*, volume 119 of *Proceedings of Machine Learning Research*, pp. 1691–1703. PMLR, 13–18 Jul 2020. URL <https://proceedings.mlr.press/v119/chen20s.html>.
- Mark Chen, Jerry Tworek, Heewoo Jun, Qiming Yuan, Henrique Ponde de Oliveira Pinto, Jared Kaplan, Harri Edwards, Yuri Burda, Nicholas Joseph, Greg Brockman, Alex Ray, Raul Puri, Gretchen Krueger, Michael Petrov, Heidy Khlaaf, Girish Sastry, Pamela Mishkin, Brooke Chan, Scott Gray, Nick Ryder, Mikhail Pavlov, Alethea Power, Lukasz Kaiser, Mohammad Bavarian, Clemens Winter, Philippe Tillet, Felipe Petroski Such, Dave Cummings, Matthias Plappert, Fotios Chantzis, Elizabeth Barnes, Ariel Herbert-Voss, William Hebgen Guss, Alex Nichol, Alex Paino, Nikolas Tezak, Jie Tang, Igor Babuschkin, Suchir Balaji, Shantanu Jain, William Saunders, Christopher Hesse, Andrew N. Carr, Jan Leike, Josh Achiam, Vedant Misra, Evan Morikawa, Alec Radford, Matthew Knight, Miles Brundage, Mira Murati, Katie Mayer, Peter Welinder, Bob McGrew, Dario Amodei, Sam McCandlish, Ilya Sutskever, and Wojciech Zaremba. Evaluating large language models trained on code, 2021. URL <https://arxiv.org/abs/2107.03374>.
- Kyunghyun Cho, Bart van Merriënboer, Çağlar Gülçehre, Dzmitry Bahdanau, Fethi Bougares, Holger Schwenk, and Yoshua Bengio. Learning phrase representations using rnn encoder-decoder for statistical machine translation. In *EMNLP*, 2014.
- Aakanksha Chowdhery, Sharan Narang, Jacob Devlin, Maarten Bosma, Gaurav Mishra, Adam Roberts, Paul Barham, Hyung Won Chung, Charles Sutton, Sebastian Gehrmann, Parker Schuh, Kensen Shi, Sasha Tsvyashchenko, Joshua Maynez, Abhishek Rao, Parker Barnes, Yi Tay, Noam Shazeer, Vinodkumar Prabhakaran, Emily Reif, Nan Du, Ben Hutchinson, Reiner Pope, James Bradbury, Jacob Austin, Michael Isard, Guy Gur-Ari, Pengcheng Yin, Toju Duke, Anselm Levskaya, Sanjay Ghemawat, Sunipa Dev, Henryk Michalewski, Xavier Garcia, Vedant Misra, Kevin Robinson, Liam Fedus, Denny Zhou, Daphne Ippolito, David Luan, Hyeontaek Lim, Barret Zoph, Alexander Spiridonov, Ryan Sepassi, David Dohan, Shivani Agrawal, Mark Omernick, Andrew M. Dai, Thanumalayan Sankaranarayanan Pillai, Marie Pellat, Aitor Lewkowycz, Erica Moreira, Rewon Child, Oleksandr Polozov, Katherine Lee, Zongwei Zhou, Xuezhi Wang, Brennan Saeta, Mark Diaz, Orhan Firat, Michele Catasta, Jason Wei, Kathy Meier-Hellstern, Douglas Eck, Jeff Dean, Slav Petrov, and Noah Fiedel. Palm: Scaling language modeling with pathways, 2022.

- Damai Dai, Yutao Sun, Li Dong, Yaru Hao, Shuming Ma, Zhifang Sui, and Furu Wei. Why can gpt learn in-context? language models implicitly perform gradient descent as meta-optimizers, 2023.
- Guy Dar, Mor Geva, Ankit Gupta, and Jonathan Berant. Analyzing transformers in embedding space, 2022.
- Jacob Devlin, Ming-Wei Chang, Kenton Lee, and Kristina Toutanova. Bert: Pre-training of deep bidirectional transformers for language understanding, 2019.
- Jeff Donahue, Lisa Anne Hendricks, Sergio Guadarrama, Marcus Rohrbach, Subhashini Venugopalan, Kate Saenko, and Trevor Darrell. Long-term recurrent convolutional networks for visual recognition and description. *CoRR*, abs/1411.4389, 2015.
- Alexey Dosovitskiy, Lucas Beyer, Alexander Kolesnikov, Dirk Weissenborn, Xiaohua Zhai, Thomas Unterthiner, Mostafa Dehghani, Matthias Minderer, Georg Heigold, Sylvain Gelly, Jakob Uszkoreit, and Neil Houlsby. An image is worth 16x16 words: Transformers for image recognition at scale. *CoRR*, abs/2010.11929, 2020.
- Danny Driess, Fei Xia, Mehdi S. M. Sajjadi, Corey Lynch, Aakanksha Chowdhery, Brian Ichter, Ayzaan Wahid, Jonathan Tompson, Quan Vuong, Tianhe Yu, Wenlong Huang, Yevgen Chebotar, Pierre Sermanet, Daniel Duckworth, Sergey Levine, Vincent Vanhoucke, Karol Hausman, Marc Toussaint, Klaus Greff, Andy Zeng, Igor Mordatch, and Pete Florence. Palm-e: An embodied multimodal language model, 2023.
- Nelson Elhage, Neel Nanda, Catherine Olsson, Tom Henighan, Nicholas Joseph, Ben Mann, Amanda Askell, Yuntao Bai, Anna Chen, Tom Conerly, Nova DasSarma, Dawn Drain, Deep Ganguli, Zac Hatfield-Dodds, Danny Hernandez, Andy Jones, Jackson Kernion, Liane Lovitt, Kamal Ndousse, Dario Amodei, Tom Brown, Jack Clark, Jared Kaplan, Sam McCandlish, and Chris Olah. A mathematical framework for transformer circuits. *Transformer Circuits Thread*, 2021. <https://transformer-circuits.pub/2021/framework/index.html>.
- Daniel Y. Fu, Tri Dao, Khaled K. Saab, Armin W. Thomas, Atri Rudra, and Christopher Ré. Hungry hungry hippos: Towards language modeling with state space models, 2023.
- Leo Gao, Jonathan Tow, Stella Biderman, Sid Black, Anthony DiPofi, Charles Foster, Laurence Golding, Jeffrey Hsu, Kyle McDonell, Niklas Muennighoff, Jason Phang, Laria Reynolds, Eric Tang, Anish Thite, Ben Wang, Kevin Wang, and Andy Zou. A framework for few-shot language model evaluation, September 2021. URL <https://doi.org/10.5281/zenodo.5371628>.
- Mor Geva, Avi Caciularu, Kevin Ro Wang, and Yoav Goldberg. Transformer feed-forward layers build predictions by promoting concepts in the vocabulary space, 2022.
- Rohit Girdhar, Alaaeldin El-Nouby, Zhuang Liu, Mannat Singh, Kalyan Vasudev Alwala, Armand Joulin, and Ishan Misra. Imagebind: One embedding space to bind them all, 2023.
- Alex Graves. Generating sequences with recurrent neural networks. *CoRR*, abs/1308.0850, 2013.
- Alex Graves. Generating sequences with recurrent neural networks, 2014.
- Albert Gu, Karan Goel, and Christopher Ré. Efficiently modeling long sequences with structured state spaces, 2022.
- Sepp Hochreiter and Jürgen Schmidhuber. Long short-term memory. *Neural Computation*, 9:1735–1780, 1997a. URL <https://api.semanticscholar.org/CorpusID:1915014>.
- Sepp Hochreiter and Jürgen Schmidhuber. Long short-term memory. *Neural Comput.*, 9(8):1735–1780, November 1997b. ISSN 0899-7667. doi: 10.1162/neco.1997.9.8.1735. URL <http://dx.doi.org/10.1162/neco.1997.9.8.1735>.
- Ari Holtzman, Jan Buys, Li Du, Maxwell Forbes, and Yejin Choi. The curious case of neural text degeneration, 2020.

- Justin Johnson, Andrej Karpathy, and Li Fei-Fei. Denscap: Fully convolutional localization networks for dense captioning. *CoRR*, abs/1511.07571, 2016.
- Nal Kalchbrenner, Ivo Danihelka, and Alex Graves. Grid long short-term memory. *CoRR*, abs/1507.01526, 2015.
- Nal Kalchbrenner, Lasse Espeholt, Karen Simonyan, Aäron van den Oord, Alex Graves, and Koray Kavukcuoglu. Neural machine translation in linear time. *CoRR*, abs/1610.10099, 2016.
- Ehud Karpas, Omri Abend, Yonatan Belinkov, Barak Lenz, Opher Lieber, Nir Ratner, Yoav Shoham, Hofit Bata, Yoav Levine, Kevin Leyton-Brown, Dor Muhlgay, Noam Rozen, Erez Schwartz, Gal Shachaf, Shai Shalev-Shwartz, Amnon Shashua, and Moshe Tenenholz. Mrkl systems: A modular, neuro-symbolic architecture that combines large language models, external knowledge sources and discrete reasoning, 2022.
- Justin Kerr, Chung Min Kim, Ken Goldberg, Angjoo Kanazawa, and Matthew Tancik. Lurf: Language embedded radiance fields. *arXiv preprint arXiv:2303.09553*, 2023.
- Takeshi Kojima, Shixiang Shane Gu, Machel Reid, Yutaka Matsuo, and Yusuke Iwasawa. Large language models are zero-shot reasoners, 2023.
- Michal Kosinski. Theory of mind may have spontaneously emerged in large language models, 2023.
- Patrick Lewis, Ethan Perez, Aleksandra Piktus, Fabio Petroni, Vladimir Karpukhin, Naman Goyal, Heinrich Küttler, Mike Lewis, Wen tau Yih, Tim Rocktäschel, Sebastian Riedel, and Douwe Kiela. Retrieval-augmented generation for knowledge-intensive nlp tasks, 2021.
- Ang Li, Allan Jabri, Armand Joulin, and Laurens van der Maaten. Learning visual n-grams from web data, 2016. URL <https://arxiv.org/abs/1612.09161>.
- Yaobo Liang, Chenfei Wu, Ting Song, Wenshan Wu, Yan Xia, Yu Liu, Yang Ou, Shuai Lu, Lei Ji, Shaoguang Mao, Yun Wang, Linjun Shou, Ming Gong, and Nan Duan. Taskmatrix.ai: Completing tasks by connecting foundation models with millions of apis, 2023.
- Yinhan Liu, Myle Ott, Naman Goyal, Jingfei Du, Mandar Joshi, Danqi Chen, Omer Levy, Mike Lewis, Luke Zettlemoyer, and Veselin Stoyanov. Roberta: A robustly optimized BERT pretraining approach. *CoRR*, abs/1907.11692, 2019.
- Jiasen Lu, Christopher Clark, Rowan Zellers, Roozbeh Mottaghi, and Aniruddha Kembhavi. Unified-io: A unified model for vision, language, and multi-modal tasks, 2022.
- Pan Lu, Baolin Peng, Hao Cheng, Michel Galley, Kai-Wei Chang, Ying Nian Wu, Song-Chun Zhu, and Jianfeng Gao. Chameleon: Plug-and-play compositional reasoning with large language models, 2023.
- Tomas Mikolov, Kai Chen, Greg Corrado, and Jeffrey Dean. Efficient estimation of word representations in vector space, 2013a. URL <https://arxiv.org/abs/1301.3781>.
- Tomás Mikolov, Ilya Sutskever, Kai Chen, Greg Corrado, and Jeffrey Dean. Distributed representations of words and phrases and their compositionality. *CoRR*, abs/1310.4546, 2013b.
- Volodymyr Mnih, Nicolas Heess, Alex Graves, and Koray Kavukcuoglu. Recurrent models of visual attention. In *NIPS*, 2014.
- Catherine Olsson, Nelson Elhage, Neel Nanda, Nicholas Joseph, Nova DasSarma, Tom Henighan, Ben Mann, Amanda Askell, Yuntao Bai, Anna Chen, Tom Conerly, Dawn Drain, Deep Ganguli, Zac Hatfield-Dodds, Danny Hernandez, Scott Johnston, Andy Jones, Jackson Kernion, Liane Lovitt, Kamal Ndousse, Dario Amodei, Tom Brown, Jack Clark, Jared Kaplan, Sam McCandlish, and Chris Olah. In-context learning and induction heads. *Transformer Circuits Thread*, 2022. <https://transformer-circuits.pub/2022/in-context-learning-and-induction-heads/index.html>.
- OpenAI. Gpt-4 technical report, 2023.

- Long Ouyang, Jeff Wu, Xu Jiang, Diogo Almeida, Carroll L. Wainwright, Pamela Mishkin, Chong Zhang, Sandhini Agarwal, Katarina Slama, Alex Ray, John Schulman, Jacob Hilton, Fraser Kelton, Luke Miller, Maddie Simens, Amanda Askell, Peter Welinder, Paul Christiano, Jan Leike, and Ryan Lowe. Training language models to follow instructions with human feedback, 2022.
- Joon Sung Park, Joseph C. O'Brien, Carrie J. Cai, Meredith Ringel Morris, Percy Liang, and Michael S. Bernstein. Generative agents: Interactive simulacra of human behavior, 2023.
- Guilherme Penedo, Quentin Malartic, Daniel Hesslow, Ruxandra Cojocaru, Alessandro Cappelli, Hamza Alobeidli, Baptiste Pannier, Ebtesam Almazrouei, and Julien Launay. The RefinedWeb dataset for Falcon LLM: outperforming curated corpora with web data, and web data only. *arXiv preprint arXiv:2306.01116*, 2023. URL <https://arxiv.org/abs/2306.01116>.
- Michael Poli, Stefano Massaroli, Eric Nguyen, Daniel Y. Fu, Tri Dao, Stephen Baccus, Yoshua Bengio, Stefano Ermon, and Christopher Ré. Hyena hierarchy: Towards larger convolutional language models, 2023.
- Alec Radford, Jong Wook Kim, Chris Hallacy, Aditya Ramesh, Gabriel Goh, Sandhini Agarwal, Girish Sastry, Amanda Askell, Pamela Mishkin, Jack Clark, Gretchen Krueger, and Ilya Sutskever. Learning transferable visual models from natural language supervision, 2021. URL <https://arxiv.org/abs/2103.00020>.
- Colin Raffel, Noam Shazeer, Adam Roberts, Katherine Lee, Sharan Narang, Michael Matena, Yanqi Zhou, Wei Li, and Peter J. Liu. Exploring the limits of transfer learning with a unified text-to-text transformer, 2020.
- Aditya Ramesh, Mikhail Pavlov, Gabriel Goh, Scott Gray, Chelsea Voss, Alec Radford, Mark Chen, and Ilya Sutskever. Zero-shot text-to-image generation. *CoRR*, abs/2102.12092, 2021a.
- Aditya Ramesh, Mikhail Pavlov, Gabriel Goh, Scott Gray, Chelsea Voss, Alec Radford, Mark Chen, and Ilya Sutskever. Zero-shot text-to-image generation, 2021b. URL <https://arxiv.org/abs/2102.12092>.
- Scott Reed, Konrad Zolna, Emilio Parisotto, Sergio Gomez Colmenarejo, Alexander Novikov, Gabriel Barth-Maron, Mai Gimenez, Yury Sulsky, Jackie Kay, Jost Tobias Springenberg, Tom Eccles, Jake Bruce, Ali Razavi, Ashley Edwards, Nicolas Heess, Yutian Chen, Raia Hadsell, Oriol Vinyals, Mahyar Bordbar, and Nando de Freitas. A generalist agent, 2022.
- Nils Reimers and Iryna Gurevych. Sentence-bert: Sentence embeddings using siamese bert-networks. In *Proceedings of the 2019 Conference on Empirical Methods in Natural Language Processing*. Association for Computational Linguistics, 11 2019. URL <https://arxiv.org/abs/1908.10084>.
- Adam Roberts, Colin Raffel, and Noam Shazeer. How much knowledge can you pack into the parameters of a language model?, 2020. URL <https://arxiv.org/abs/2002.08910>.
- Timo Schick, Jane Dwivedi-Yu, Roberto Dessì, Roberta Raileanu, Maria Lomeli, Luke Zettlemoyer, Nicola Cancedda, and Thomas Scialom. Toolformer: Language models can teach themselves to use tools, 2023.
- Sumeet S. Singh. The transformer algorithm. <https://slideslive.com/38970769?slide=35>, 2021. Invited Talk: Weaving AI Into Education, pp. 36-38.
- Marijn F. Stollenga, Wonmin Byeon, Marcus Liwicki, and Jürgen Schmidhuber. Parallel multi-dimensional lstm, with application to fast biomedical volumetric image segmentation. In *NIPS*, 2015.
- Yutao Sun, Li Dong, Shaohan Huang, Shuming Ma, Yuqing Xia, Jilong Xue, Jianyong Wang, and Furu Wei. Retentive network: A successor to transformer for large language models, 2023.
- Ilya Sutskever, Oriol Vinyals, and Quoc V Le. Sequence to sequence learning with neural networks. In Z. Ghahramani, M. Welling, C. Cortes, N. Lawrence, and K.Q. Weinberger (eds.), *Advances in Neural Information Processing Systems*, volume 27. Curran Associates, Inc., 2014. URL <https://proceedings.neurips.cc/paper/2014/file/a14ac55a4f27472c5d894ec1c3c743d2-Paper.pdf>.

- Lucas Theis and Matthias Bethge. Generative image modeling using spatial lstms. In C. Cortes, N. Lawrence, D. Lee, M. Sugiyama, and R. Garnett (eds.), *Advances in Neural Information Processing Systems*, volume 28. Curran Associates, Inc., 2015a. URL <https://proceedings.neurips.cc/paper/2015/file/2b6d65b9a9445c4271ab9076ead5605a-Paper.pdf>.
- Lucas Theis and Matthias Bethge. Generative image modeling using spatial lstms. In *NIPS*, 2015b.
- Aäron van den Oord, Sander Dieleman, Heiga Zen, Karen Simonyan, Oriol Vinyals, Alex Graves, Nal Kalchbrenner, Andrew W. Senior, and Koray Kavukcuoglu. Wavenet: A generative model for raw audio. *CoRR*, abs/1609.03499, 2016a.
- Aäron van den Oord, Nal Kalchbrenner, and Koray Kavukcuoglu. Pixel recurrent neural networks. *CoRR*, abs/1601.06759, 2016b.
- Aäron van den Oord, Nal Kalchbrenner, and Koray Kavukcuoglu. Pixel recurrent neural networks. In *ICML*, 2016c.
- Aäron van den Oord, Nal Kalchbrenner, Oriol Vinyals, Lasse Espeholt, Alex Graves, and Koray Kavukcuoglu. Conditional image generation with pixelcnn decoders. *CoRR*, abs/1606.05328, 2016d.
- Ali Vardasbi, Telmo Pessoa Pires, Robin M. Schmidt, and Stephan Peitz. State spaces aren't enough: Machine translation needs attention, 2023.
- Ashish Vaswani, Noam Shazeer, Niki Parmar, Jakob Uszkoreit, Llion Jones, Aidan N. Gomez, Lukasz Kaiser, and Illia Polosukhin. Attention is all you need. *CoRR*, abs/1706.03762, 2017.
- Johannes von Oswald, Eyvind Niklasson, Ettore Randazzo, João Sacramento, Alexander Mordvintsev, Andrey Zhmoginov, and Max Vladymyrov. Transformers learn in-context by gradient descent, 2023.
- Jason Wei, Yi Tay, Rishi Bommasani, Colin Raffel, Barret Zoph, Sebastian Borgeaud, Dani Yogatama, Maarten Bosma, Denny Zhou, Donald Metzler, Ed H. Chi, Tatsunori Hashimoto, Oriol Vinyals, Percy Liang, Jeff Dean, and William Fedus. Emergent abilities of large language models, 2022a.
- Jason Wei, Xuezhi Wang, Dale Schuurmans, Maarten Bosma, Brian Ichter, Fei Xia, Ed Chi, Quoc Le, and Denny Zhou. Chain of thought prompting elicits reasoning in large language models, 2022b. URL <https://arxiv.org/abs/2201.11903>.
- Thomas Wolf, Lysandre Debut, Victor Sanh, Julien Chaumond, Clement Delangue, Anthony Moi, Pierric Cistac, Tim Rault, Rémi Louf, Morgan Funtowicz, Joe Davison, Sam Shleifer, Patrick von Platen, Clara Ma, Yacine Jernite, Julien Plu, Canwen Xu, Teven Le Scao, Sylvain Gugger, Mariama Drame, Quentin Lhoest, and Alexander M. Rush. Huggingface's transformers: State-of-the-art natural language processing, 2020.
- Kelvin Xu, Jimmy Ba, Jamie Ryan Kiros, Kyunghyun Cho, Aaron C. Courville, Ruslan Salakhutdinov, Richard S. Zemel, and Yoshua Bengio. Show, attend and tell: Neural image caption generation with visual attention. In *ICML*, 2015.
- Shunyu Yao, Jeffrey Zhao, Dian Yu, Nan Du, Izhak Shafran, Karthik Narasimhan, and Yuan Cao. React: Synergizing reasoning and acting in language models, 2023.
- Rowan Zellers, Ari Holtzman, Yonatan Bisk, Ali Farhadi, and Yejin Choi. Hellaswag: Can a machine really finish your sentence?, 2019.

## A APPENDIX

### A.1 ATTENTION LAYER MATH

First we show that the attention layer output can be recast as a sum of outputs of individual heads i.e., each attention head works independently and in parallel with other heads. All vectors are represented as rows.

$$\begin{aligned}
 H & : \text{ number of heads} \\
 d & : \text{ vector dimension of heads } = D/H \\
 A_h & : n \times m \text{ attention matrix of head } h, \text{ rows sum to } 1 \\
 V_h & = m \times d \text{ value vectors of head } h \\
 \mathbf{W}_o & : D \times D \text{ output projection matrix} \\
 \mathbf{W}_{o,h} & : d \times D ; h^{th} \text{ of } H \text{ row-wise slices of } \mathbf{W}_o \text{ where} \\
 O & : n \times D \text{ attention layer output vectors} \\
 & = [A_1 V_1 \quad \cdots \quad A_H V_H] \mathbf{W}_o \\
 & = [A_1 V_1 \quad \cdots \quad A_H V_H] \begin{bmatrix} \mathbf{W}_{o,1} \\ \cdots \\ \mathbf{W}_{o,H} \end{bmatrix} \\
 & = \sum_h A_h V_h \mathbf{W}_{o,h} \\
 \text{defining } O_h & = A_h V_h \mathbf{W}_{o,h} ; n \times d \text{ output of head } h \\
 \text{we get } O & = \sum_h O_h
 \end{aligned}$$

We show next that each head can be viewed as an independent linear transform of input vectors  $x_i$  without any interaction with other vectors i.e, filtering, followed by soft-clustering i.e., matrix multiplication with  $A_h$ .

$$\begin{aligned}
 \mathbf{X} & : \begin{bmatrix} x_1 \\ x_2 \\ \cdots \\ x_n \end{bmatrix} ; n \times D \text{ matrix of row vectors (inputs); } n = \text{ sequence length} \\
 \mathbf{W}_{v,h} & : D \times d \text{ value projection matrix of head } h \\
 V_h & = \mathbf{X} \mathbf{W}_{v,h} \\
 O_h & = A_h V_h \mathbf{W}_{o,h} \\
 & = A_h \mathbf{X} (\mathbf{W}_{v,h} \mathbf{W}_{o,h}) \\
 & = A_h \mathbf{X} (\mathbf{W}_{vo,h}) ; \mathbf{W}_{vo,h} = \mathbf{W}_{v,h} \mathbf{W}_{o,h} \in R^{D \times D} \\
 & = A_h \begin{bmatrix} x_1 \mathbf{W}_{vo,h} \\ x_2 \mathbf{W}_{vo,h} \\ \cdots \\ x_n \mathbf{W}_{vo,h} \end{bmatrix} \\
 & = A_h \text{ filter}_{\mathbf{W}_{vo,h}}(\mathbf{X})
 \end{aligned}$$

For completeness sake, derivations of  $A_h$  are shown below.

$$\begin{aligned}
\mathbf{W}_{q,h} &: D \times d \text{ query projection matrix of head } h \\
\mathbf{W}_{k,h} &: D \times d \text{ key projection matrix of head } h \\
Q_h &= \mathbf{X}\mathbf{W}_{q,h}; n \times d \text{ query vectors of head } h \\
K_h &= \mathbf{X}\mathbf{W}_{k,h}; m \times d \text{ key vectors of head } h \\
B &: n \times m \text{ position bias; absolute or relative, including ROPE} \\
A_h &: n \times m \text{ attention matrix for head } h, \text{ rows sum to 1} \\
&= \text{softmax}(Q_h K_h^T + B); \text{ softmax over columns i.e., } \dim = 1 \\
&= \text{softmax}(\mathbf{X}\mathbf{W}_{q,h}\mathbf{W}_{k,h}^T\mathbf{X}^T + B) \\
&= \text{softmax}(\mathbf{X}\mathbf{W}_{qk,h}\mathbf{X}^T + B); \mathbf{W}_{qk,h} = \mathbf{W}_{q,h}\mathbf{W}_{k,h}^T \\
&= \text{softmax}(\text{filter}_{\mathbf{W}_{qk,h}}(\mathbf{X})\mathbf{X}^T + B)
\end{aligned}$$

## A.2 ADDITIONAL SIMILARITY MAPS

Additional similarity maps for the following sample are shown in 12.

Below is a listing of the sample used to produce the similarity maps.

Grade answers

Q:

Give three pairs of pixel values  $(x, y) = [[?, ?, ?]]$  and  $(x+1, y) = [[?, ?, ?]]$  in t

### Pair 1

$(x, y) =$

$(x+1, y) =$

### Pair 2

$(x, y) =$

$(x+1, y) =$

### Pair 3

$(x, y) =$

$(x+1, y) =$

R:

1: All Correct - Average of first array must be  $\geq$  second (5.0)

2: Example 1 incorrect (0.0)

3: Example 2 incorrect (0.0)

4: Example 3 incorrect (0.0)

5: Impossible pixel values,  $>1$  (0.0)

A:

[5, 6, 7]

[2, 3, 4]

[4, 5, 6]

[2, 3, 4]

[7, 8, 9]

[3, 4, 5]

G: 00001

L: 000

A:

[3, 4, 5]

[2, 3, 4]

[4, 5, 6]

[3, 4, 5]

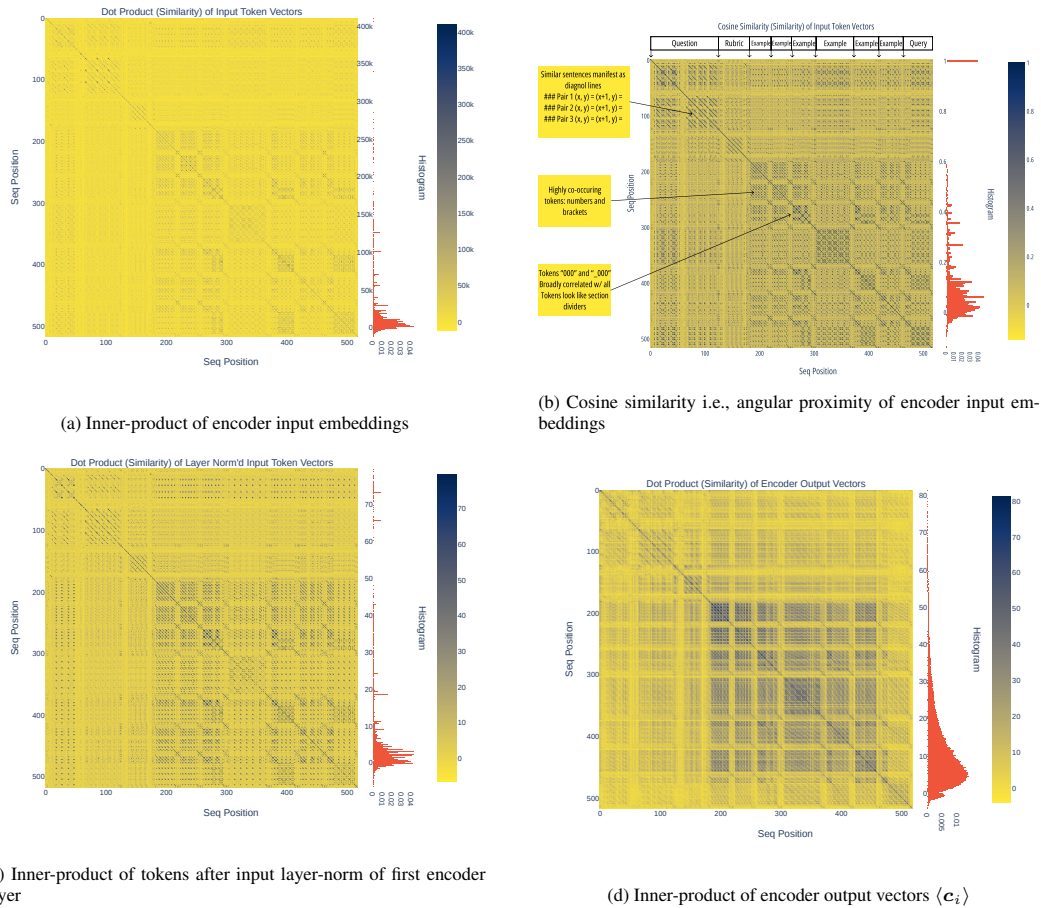


Figure 11: Vector similarity maps for the same example as in Fig. 3, but passed through a frozen google/flan-t5-xxl model. The structure of the document and similarity of associated tokens is still clearly visible despite the fact that the model is a generic pretrained model. The fact that the patterns are more visible by cosine-similarity indicates that associated tokens (such as brackets and numbers) cluster together in Embedding Space based on angular separation. Subfigure (d) shows a similar map of the encoder output. The patterns are fuzzier but still match up with the first layer indicating that encoded composite vectors still retain their original identity which is not surprising since it's trained to predict the input token.

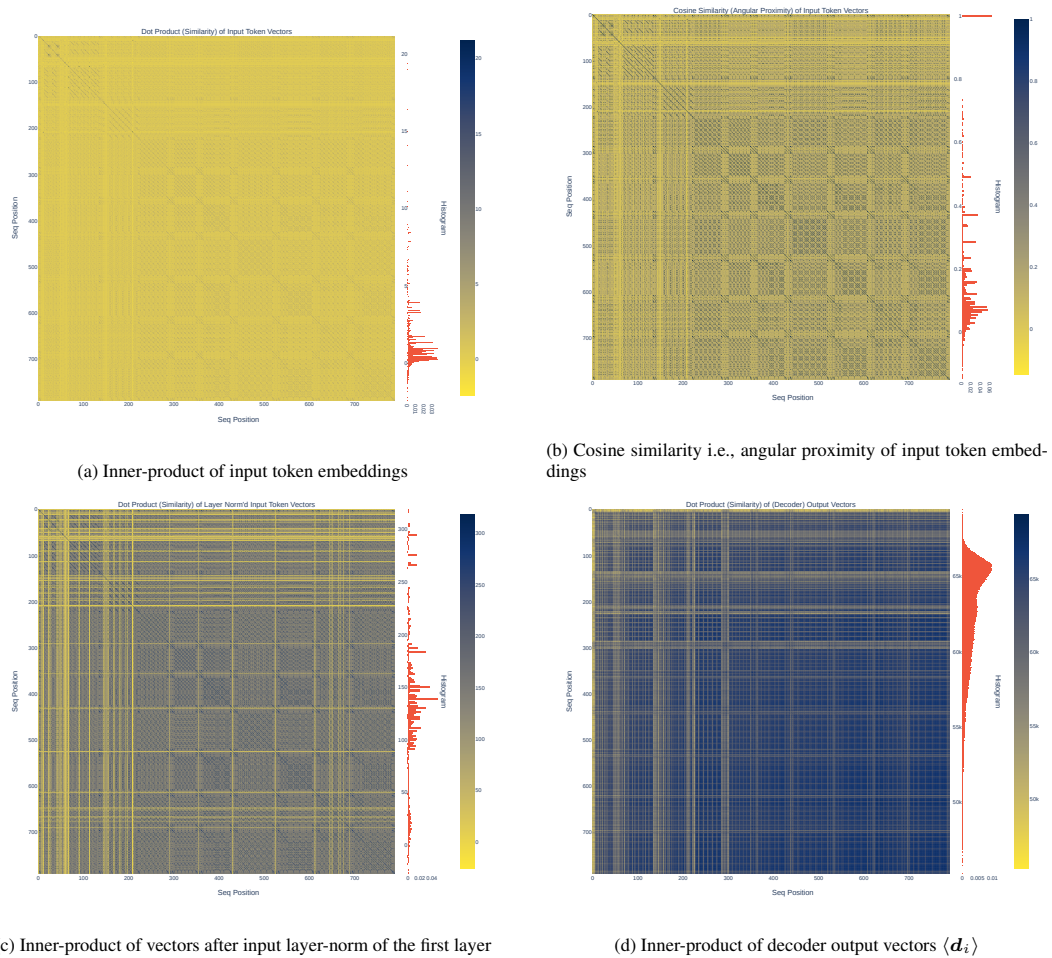


Figure 12: Vector similarity maps for the same input as Fig. 3, but passed through a frozen tiuae/falcon-7b model. The structure of the document and similarity of associated tokens is still clearly visible despite the fact that the model is a generic pretrained model. The fact that the patterns are more visible by cosine-similarity indicates that associated tokens (such as brackets and numbers) cluster together in Embedding Space based on angular separation. Subfigure (d) shows a similar map of the decoder output. The patterns are fuzzier than its encoder stack (T5 and FlanT5) counterparts indicating that there’s more mixing in the decoder stack which is not surprising since it’s trained to predict a different token than the input.

[5, 6, 7]  
[4, 5, 6]

G: 00001  
L: 000

A:  
[2, 2, 2]  
[1, 1, 1]  
[2, 2, 2]  
[0.2, 0.2, 0.2]  
[2, 2, 2]  
[0.3, 0.3, 0.3]

G: 10000  
L: 1

A:  
[.8, .8, .8]  
[.3, .3, .3]  
[.8, .8, .8]  
[.8, .8, .8]  
[.7, .7, .1]  
[.3, .3, .3]

G: 10000  
L: 1

A:  
[2, 2, 2]  
[1, 1, 1]  
[0.6, 0.6, 0.6]  
[0.3, 0.3, 0.3]  
[0.7, 0.7, 0.7]  
[0.4, 0.4, 0.4]

G: 10000  
L: 1

A:  
[2, 1, 1]  
[1, 1, 1]  
[24, 46, 61]  
[2, 2, 2]  
[22, 51, 2]  
[21, 3, 1]

G: 00001  
L: 000

A:  
[2, 2, 2]  
[1, 1, 1]  
[0.6, 0.8, 0.9]  
[0.2, 0.3, 0.4]  
[0.8, 0.5, 0.6]  
[0.3, 0.3, 0.4]

G:

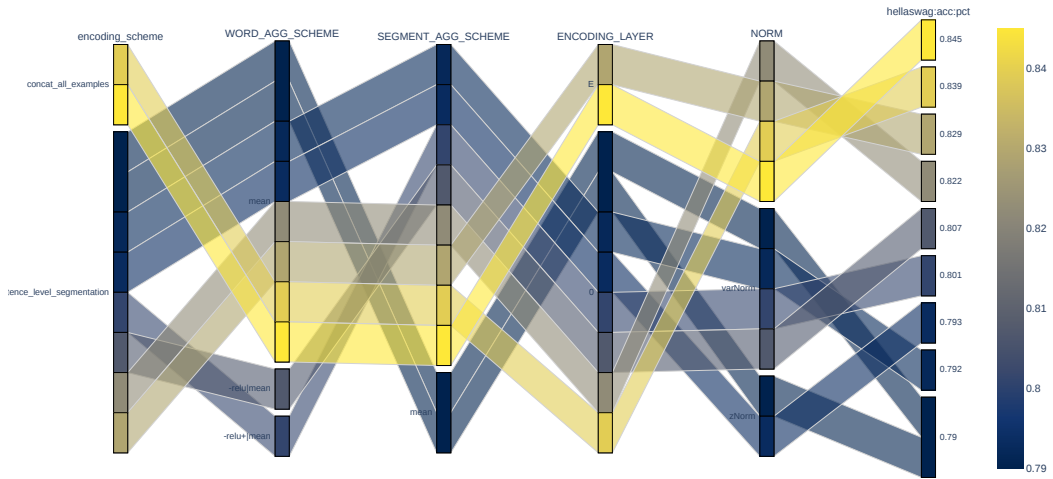
L:

### A.3 CONCEPT COMPOSITION SCHEMES

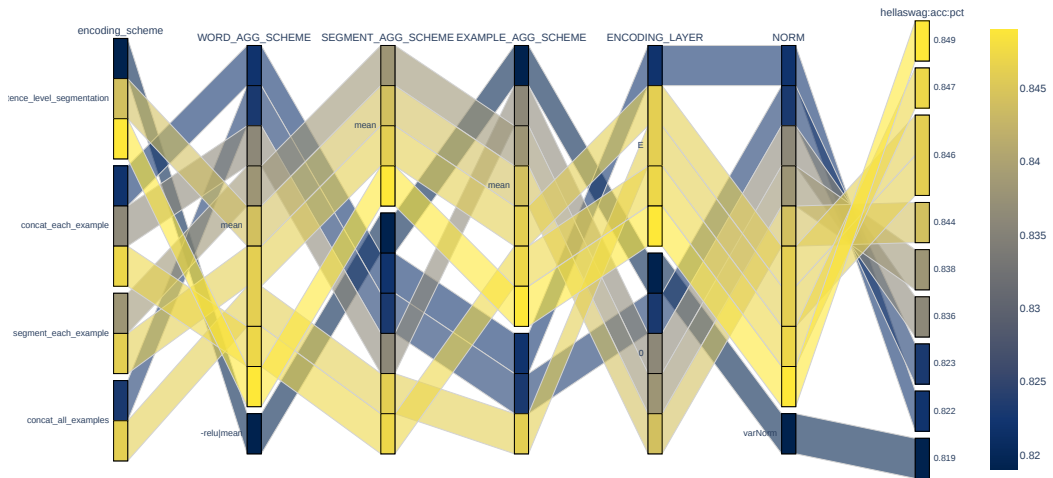
Permutations of the following parameters were used to generate the distributed concept composition schemes that we swept over:

1. Encoding Scheme, denoted *encoding\_scheme*. The overall scheme of distributed encoding. Possible values:
  - (a) *sentence\_level\_segmentation*: Segment the context into individual sentences. These then get encoded via the transformer stack based on the ENCODING\_LAYER parameter, yielding a sequence of embedded tokens which are then aggregated (or not) based on the SEGMENT\_AGG\_SCHEME parameter and so on.
  - (b) *segment\_each\_example*: Segment each example of the context into its individual sections. For Hellaswag this means, 1) the context passage and 2) the completion passage. *merge\_all\_segments*: Each example is segmented same as in *segment\_each\_example*, then all segments across all examples are merged into one single 'example'. Doing so circumvents EXAMPLE\_AGG\_SCHEME (but not SEGMENT\_AGG\_SCHEME), since now there's only one example.
  - (c) *concat\_each\_example*: Each example's text is considered a single segment.
  - (d) *concat\_all\_examples*: All examples of the context are concatenated into a single sequence which is considered as the one segment of the entire context.
  - (e) *cross-encoding*: This is the standard way of running a transformer, with no aggregation at any level. A token-sequence is input and a token-sequence is output.
2. *ENCODING\_LAYER*: The Transformer stack layer from where to extract the token embedding vector. In case of encoder-decoder models, this refers to the encoder stack. In case of decoder-only models, there's only one stack. Possible values:
  - (a) *E*: Token embedding vector obtained from the input embedding matrix.
  - (b) A positive integer *l*: Implies the layer whose hidden state is used as token embedding. For an  $N$  layer stack, there are  $N + 1$  possible values, one per layer in the range  $0 - (N - 1)$  and  $N$  denoting the top of the stack (after final layer norm). Hidden state of a layer is typically its input. In the case of decoder-only models like gpt2 that use a single global position encoding, layer 0's (first layer) hidden activation = token vectors  $\langle w_i \rangle$  (i.e., 'E') + global position encodings.
  - (c) A negative integer  $-l$ : Layer number from the top, e.g. -1 means the the top of the stack i.e., the final hidden activation.
  - (d) *middle*: The middle layer of the stack.
3. *OUT\_ENCODING\_LAYER*: Applicable only to Experiment 2: Concept Similarity. The ENCODING\_Layer for the choice sequences.
4. Normalization, denoted *NORM*: Applied to vectors after an aggregation operation. Possible values:
  - (a) *None*: No normalization.
  - (b) *L2*: L2 vector-norm.
  - (c) *varNorm*: normalize vector to have unit variance.
  - (d) *zNorm*: Normalize to zero mean and unit-variance.
5. Word aggregation scheme (denoted *WORD\_AGG\_SCHEME*) used to aggregate (possibly contextualized) embedded token vectors. Possible values:
  - (a) *mean*: elementwise mean across aggregated vectors.
  - (b) *wlmean*: weighted elementwise mean across aggregated vectors. Weight of vector at position  $t$  is  $t/N$  where  $N$  is the sequence length.
  - (c) *relu|mean* - pass the vector through the feed-forward layer's activation function and then perform *mean*. Usually the activation function is a relu, gelu or similar function depending on the model.

- (d) *-relu|mean*: same as above except the activation function is reflected about the y-axis i.e.,  $-\text{relu}(-x)$ . Now it let's the negative values pass instead of the positive ones.
  - (e) *relu+|\**, *-relu+|\**: similar to *relu|\** and *-relu|\** respectively except that the original vector is added to the filtered vector (i.e.,  $\text{relu}(e)$ ) before being sent on to the next step (mean or w1mean).
  - (f) *relu|mean*
  - (g) *last*: Take the last vector  $\mathbf{d}_T$  of the sequence  $\langle \mathbf{d}_t \rangle_1^T$  as the aggregated vector. This applies to decoder-only models which apply causal masking.
6. *OUT\_WORD\_AGG\_SCHEME*: Applicable only to Experiment 2: Concept Similarity. *WORD\_AGG\_SCHEME* for the choice sequences.
  7. Segment aggregation scheme, denoted *SEGMENT\_AGG\_SCHEME*. How to aggregate embedded segment vectors of an example. Applies when there are more than one segments in an example. Possible values are:
    - (a) *mean*: Vector mean (elementwise).
    - (b) *None*: No aggregation. The segment vector sequence stays untouched and is then passed on to the *EXAMPLE\_AGG\_SCHEME*.
  8. *EXAMPLE\_AGG\_SCHEME*: Example aggregation scheme. How to aggregate embedded example vectors. Applies when there are more than one examples in the context. Possible values:
    - (a) *mean*: Vector mean (elementwise).
    - (b) *None*: The input vector sequence is passed on unaltered.
    - (c) *soft.cluster*: A weighted vector-mean with weights = soft-maxed of dot-product similarity with a choice vector. This implies a different set of weights per choice sequence.
  9. Similarity Function, denoted *SIMILARITY\_FUNC*. The function used to compare vectors in Experiment 2. Possible values:
    - (a) *dot-product*: Inner product of vectors.
    - (b) *cosine-similarity*: Cosine similarity of vectors.
    - (c) *None*: Where it's not applicable, i.e., in Experiment 1: Pyramidal Generation.

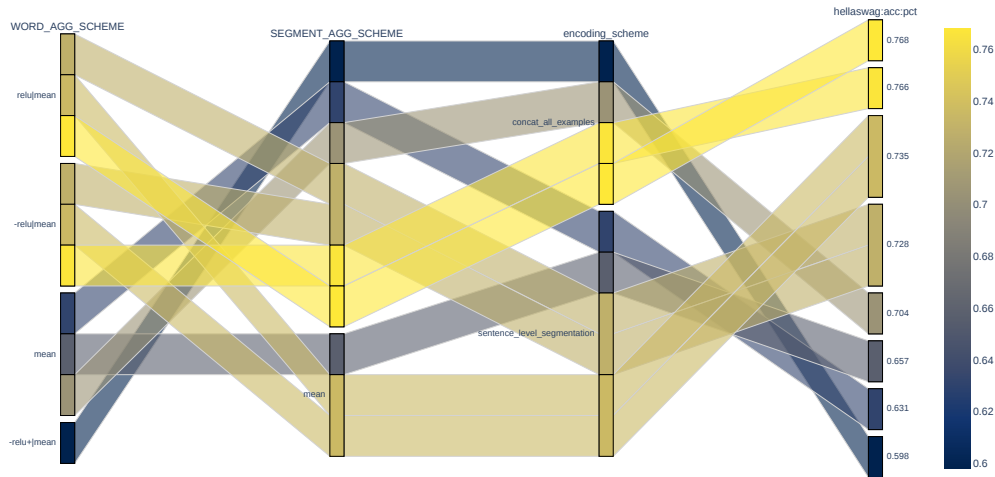


(a) zero-shot

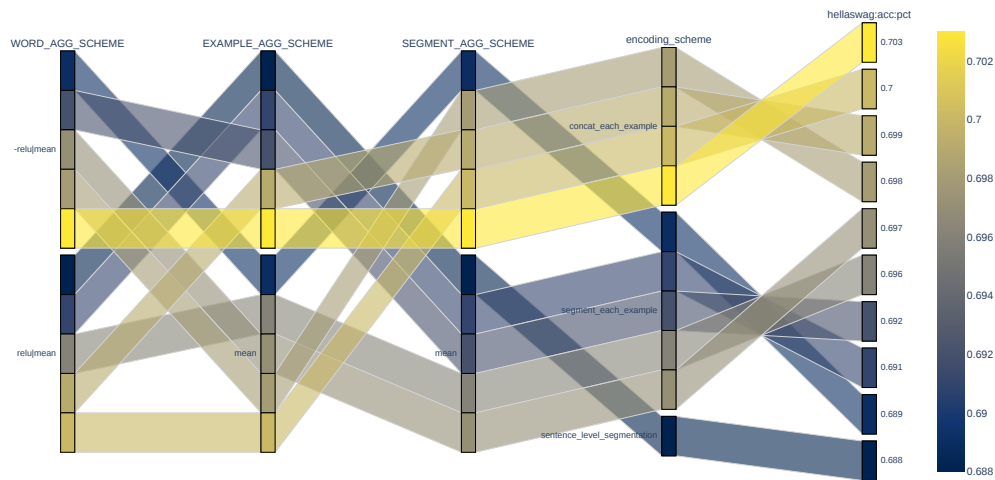


(b) 5-shot

Figure 13: Top performing 10 distributed composition schemes respectively for zero-shot (K=0) and few-shot (K=5) Pyramidal Generation experiments (test 1) for model EleutherAI/gpt-neo-1.3B. The top values are around 85% normalized Hellaswag accuracy score (denoted hellaswag:acc:pct).

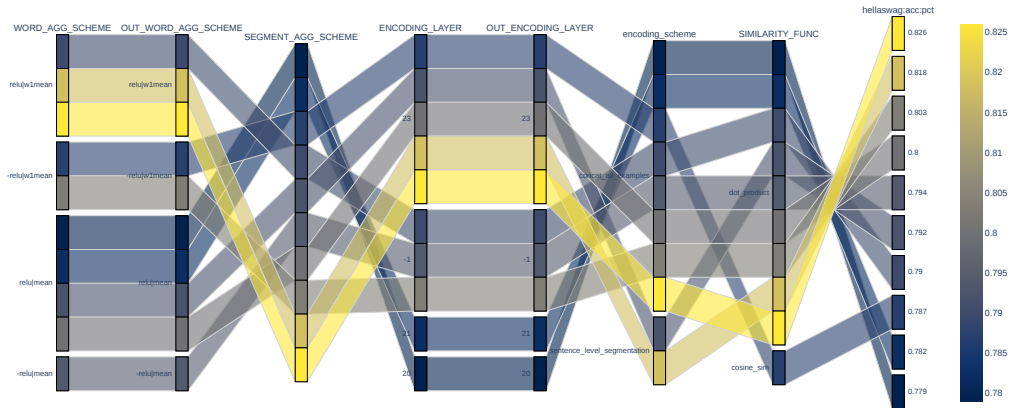


(a) zero-shot, EXAMPLE\_AGG\_SCHEME=None, ENCODING\_LAYER=-1, NORM=None

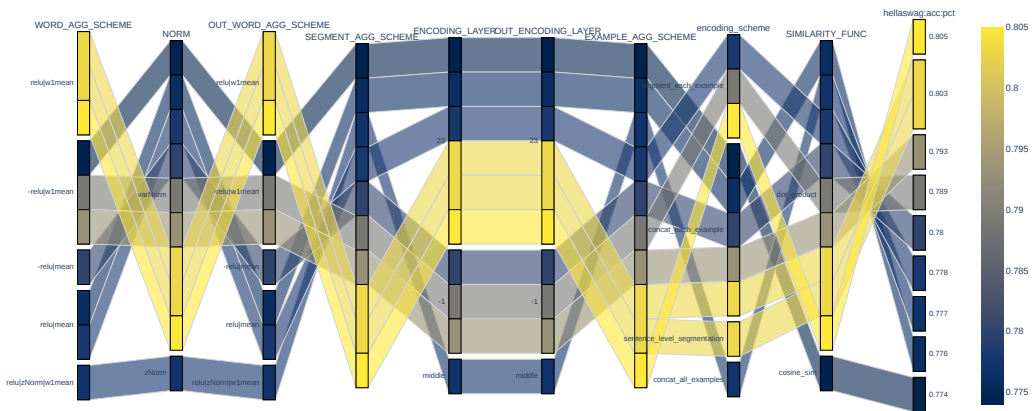


(b) 5-shot, ENCODING\_LAYER=-1, NORM=None

Figure 14: Top performing 10 distributed composition schemes respectively for zero-shot (K=0) and few-shot (K=5) Pyramidal Generation experiments for model google/flan-t5-xl. hellaswag:acc:pct stands for the normalized Hellaswag score reported by the test run.

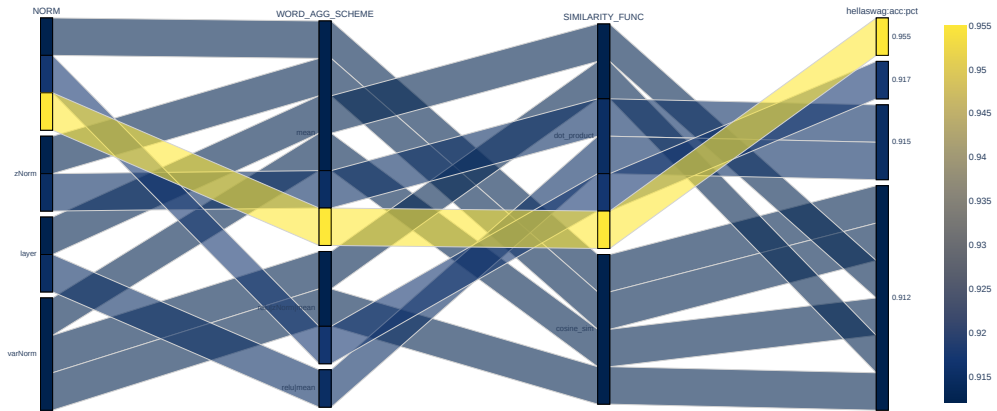


(a) zero-shot. NORM=varNorm,EXAMPLE\_AGG\_SCHEME=None

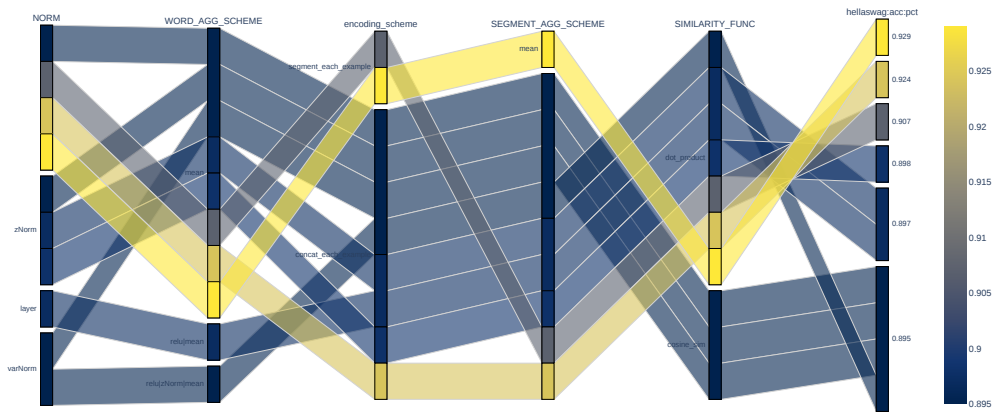


(b) 5-shot

Figure 15: Top performing 10 distributed composition schemes of test 2 for model EleutherAI/gpt-neo-1.3B. hellaswag:acc:pct stands for the normalized Hellaswag score reported by the test run.



(a) zero-shot, EXAMPLE\_AGG\_SCHEME=None, ENCODING\_LAYER=-1, encoding\_scheme=concat\_all\_examples, SEGMENT\_AGG\_SCHEME=None



(b) 5-shot, ENCODING\_LAYER=-1, NORM=None

Figure 16: Top performing 10 distributed composition schemes of test 2 for model google/flan-t5-xl. hellaswag:acc:pct stands for the normalized Hellaswag score reported by the test run.